Marine Geophysical Research (2025) 46:35
https://doi.org/10.1007/s11001-025-09596-1

ORIGINAL RESEARCH PAPER

Morphotectonics of the Gulf of Patti (Southern Tyrrhenian Sea) through pseudo-3D geophysical techniques

Giuseppe Lo Mauro[1,2] · Luca Gasperini[1] · Tiziana Sgroi[3] · Graziella Barberi[4] · Alina Polonia[1]

Received: 14 July 2025 / Accepted: 11 October 2025
© The Author(s) 2025

Abstract

The Aeolian-Tindari-Letojanni Fault System (ATLFS) is a major tectonic transfer zone extending from the Sicilian coast to the Aeolian Islands through the Gulf of Patti. It is characterized by intense seismicity, including moderate to strong historical earthquakes. The ATLFS is considered the shallow expression of the Subduction-Transform Edge Propagator (STEP) fault, which marks the southwestern termination of the Calabrian slab. Recent studies interpret the neotectonic features in the Gulf as resulting from a dextral stepover between ATLFS segments, but the geometry and activity of major faults within this depression remain uncertain. To clarify these aspects, we built a pseudo-3D tectonic model from a dense grid of seismic reflection profiles integrated with morpho-bathymetric and seismological data. Our results reveal a broad deformation zone controlling a composite sedimentary basin, where pull-apart depressions are formed by overstepping transtensional faults that cut across the Calabrian Arc causing localized subsidence superimposed on regional uplift. This configuration supports the presence, at deeper crustal and mantle levels, of a lithospheric structure acting as a STEP fault developed after the necking of the Calabrian slab.

Keywords Gulf of Patti · Calabro-Peloritani arc · Southern tyrrhenian sea · Neotectonics · Earthquakes · Pseudo-3D geophysical techniques

Introduction

The Gulf of Patti is the offshore counterpart of a sedimentary basin located at the southwestern termination of the Calabrian slab, which represents an active fragment of the northwest-dipping Western Mediterranean Subduction Zone (WMSZ; Fig. 1). This subduction zone, formed as a result of the convergence between the African and Eurasian plates, has migrated southeastward since 30 Ma due to the slab rollback process (Faccenna et al. 2004; Rosenbaum and Lister 2004; Fig. 1c).

At the edges of the migrating lower plate, variations in deformation rates have induced lithospheric wrenching and tearing at depth, accommodated by deep-rooted lithospheric faults known as Subduction-Transform Edge Propagator (STEP) faults (Govers and Wortel 2005). These tears in the lower plate generate broad deformation zones within the upper plate. In the Ionian domain, a dextral shear zone encompasses several fault systems (Polonia et al. 2016; Fig. 1b), among which the potential shallow expression of the STEP fault has been the focus of considerable debate.

Several authors have suggested that the Aeolian-Tindari-Letojanni Fault System (ATLFS) —a transtensional strike-slip fault system crossing the Peloritani Mountains and the Gulf of Patti (Fig. 1a, b)— represents the surface expression of the STEP fault along the southwestern edge of the slab (Barreca et al. 2019; Palano et al. 2015; Scarfì et al. 2018). However, the link between upper plate deformations and slab dynamics remains poorly constrained.

The northern sector of the ATLFS is also among the most seismically active regions in the southern Tyrrhenian Sea

✉ Giuseppe Lo Mauro
giuseppelomauro@cnr.it

1 Consiglio Nazionale delle Ricerche, Istituto di Scienze Marine CNR- ISMAR, Bologna, Italy

2 Dipartimento di Scienze della Terra e Geoambientali, Università di Bari, Bari, Italy

3 Istituto Nazionale di Geofisica e Vulcanologia, Sezione Roma 2, Roma, Italy

4 Istituto Nazionale di Geofisica e Vulcanologia, Osservatorio Etneo, Catania, Italy

Published online: 23 October 2025

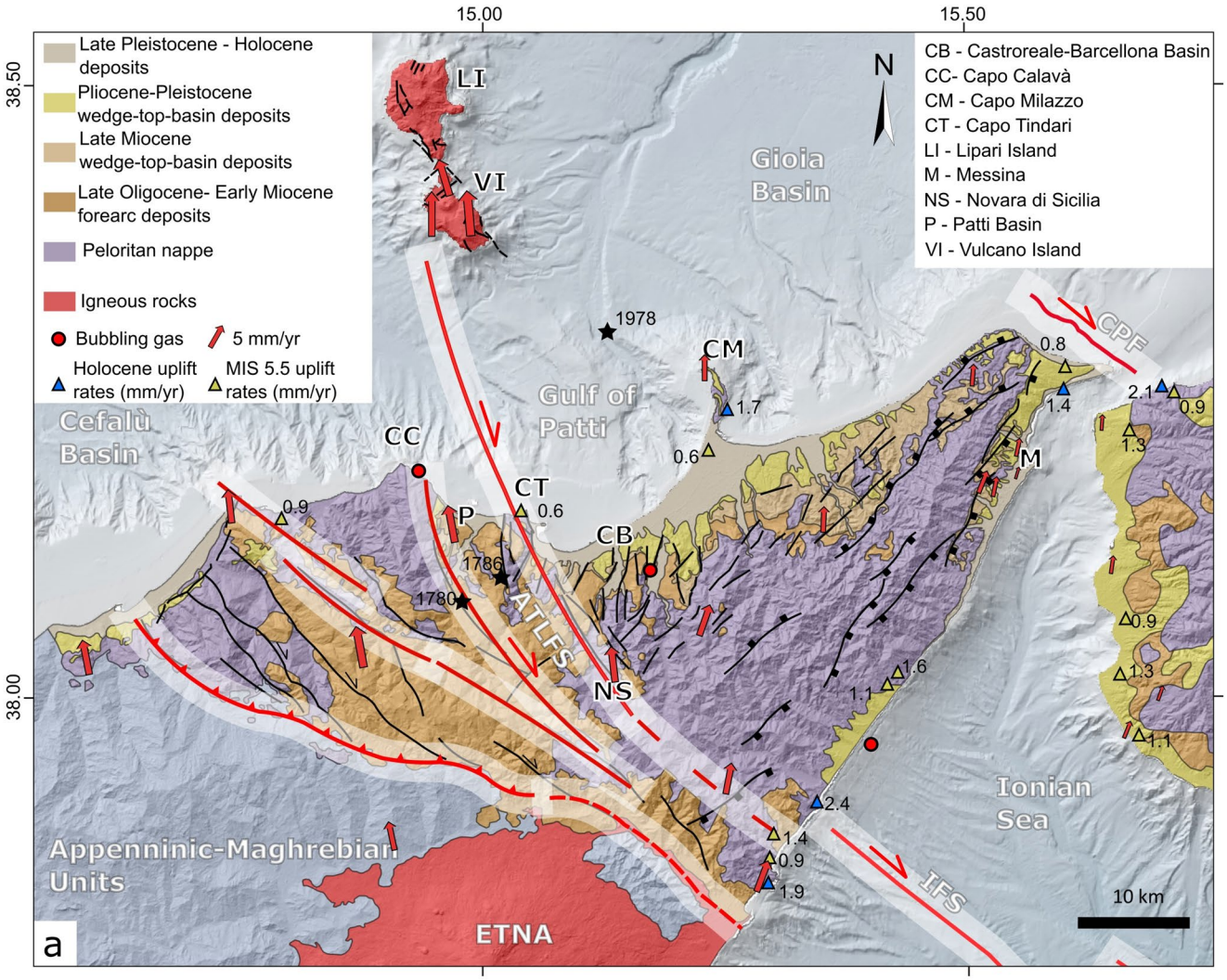
15.00
15.50
38.50
38.00
Late Pleistocene - Holocene deposits
Pliocene-Pleistocene wedge-top-basin deposits
Late Miocene wedge-top-basin deposits
Late Oligocene- Early Miocene forearc deposits
Peloritan nappe
Igneous rocks
Bubbling gas
5 mm/yr
Holocene uplift rates (mm/yr)
MIS 5.5 uplift rates (mm/yr)
CB - Castroreale-Barcellona Basin
CC- Capo Calavà
CM - Capo Milazzo
CT - Capo Tindari
LI - Lipari Island
M - Messina
NS - Novara di Sicilia
P - Patti Basin
VI - Vulcano Island
N
LI
VI
Gioia Basin
Gulf of Patti
Cefalù Basin
Appenninic-Maghrebian Units
Ionian Sea
ETNA
CC
CT
P
CB
CM
M
NS
1978
1786
1780
ATLFS
CPF
IFS
0.9
0.6
1.7
0.8
1.4
2.1
0.9
1.3
0.9
1.3
1.1
1.6
1.1
2.4
1.4
0.9
1.9
10 km
a
12.3
15.3
18.3
N
39.0
36.0
450 km
400 km
300 km
200 km
100 km
ATLFS
CPF
Calabrian arc
CEFS
Appenninic Maghrebian Chain
ETNA
IFS
AEFS
SRFS
Foreland
80 km
b
Eurasia
Africa
WMSZ
IS
30-18 Ma
BS
15-8 Ma
TS
6 Ma
5-2 Ma
0 Ma
BS - Balearic Sea
TS - Tyrrhenian Sea
IS - Ionian Sea
WMSZ - Western Mediterranean Subduction Zone
Oceanic basins
Back-arc oceanic basins
Alpine-Betic-Dinarides Hellenides belts
Appennines Maghrebides belts
c

Fig. 1 (**a**) Geological setting of the Peloritani Mountains, modified from Lentini and Carbone (2014), Pavano et al. (2015), Palano et al. (2015), and Henriquet et al. (2020). Tectonic features of the Aeolian Islands and the onshore region of the Gulf of Patti are based on Billi et al. (2006); Barreca et al. (2014); Cultrera et al. (2017a, b). GPS velocity vectors, referenced to a fixed Eurasia frame, are from Billi et al. (2023), while gas emission locations are from Italiano et al. (2019). Holocene uplift rates are from Antonioli et al. (2006), and Marine Isotope Stage (MIS) 5.5 uplift data from Ferranti et al. (2006) and Antonioli et al. (2009). Black stars indicate earthquake epicenters from Rovida et al. (2022). (**b**) Geodynamic setting of the Central Mediterranean region. IFS: Ionian Fault System (Polonia et al. 2016); AEFS: Alfeo-Etna Fault System (Polonia et al. 2016); CPF: Capo Peloro Fault, modified from Doglioni et al. (2012); ATLFS: Aeolian-Tindari-Letojanni Fault System (Palano et al. 2012). Slab isodepths are modified from Selvaggi and Chiarabba (1995). Blue arrows represent the Africa-Eurasia relative motion vector. The black line with saw teeth indicates the hinge of the slab currently subducting below the Calabrian arc. (**c**) Tectonic evolution of the western-central Mediterranean region over the past 30 Ma, modified from Chizzini et al. (2022)

and has experienced several moderate to strong earthquakes in recent history, including events in 1780 (Mw = 5.33), 1786 (Mw = 6.14), and 1978 (Mw = 6.03) (Rovida et al. 2022; Fig. 1a). This region is characterized by rough geomorphology both onshore and offshore where a narrow continental shelf, steep slopes and canyons bounding morphological highs make the region prone to gravitational instability process. The combination of this complex geological setting with the high population density on the Sicilian coast along the gulf highlights the need to accurately describe the morphostructural setting of the area in order to develop reliable hazard scenarios.

Although the tectonic setting of the onshore area around the Gulf has been described in considerable detail (Billi et al. 2006; Cultrera et al. 2017a; De Guidi et al. 2013), and a general tectonic framework has been proposed in previous studies (Cultrera et al. 2017a, b), several questions regarding the structural framework and its link to upper plate dynamics remain unresolved.

Major uncertainties persist regarding:

- the relationship between the ATLFS and other strike-slip crustal tectonic features within the broad deformation zone at the top of the southwestern edge of the Ionian slab following the slab necking process;
- the origin of observed morphological highs, namely the sill separating the Gioia and Cefalù basins, in a region dominated by transcurrent/transtensional deformation;
- the geometry of active faults in the Gulf of Patti, which controls seismicity and determines the maximum expected magnitude of future major earthquakes.

To try to answer these questions, we conducted a multiscale investigation of the Gulf of Patti. A detailed morpho-structural analysis of the Gulf was carried out using a dense grid of multichannel seismic profiles that allowed us to construct a pseudo-3D tectonic model of the subsurface reaching depths of approximately 1 km. The pseudo-3D model was integrated with morphobathymetric and chirp sonar acoustic images for near-surface structures, as well as with relocated earthquake data recorded by a combined land and ocean bottom seismometers (OBSs) seismic network to study and describe the deeper (crustal to mantle) portion of the fault system and its link with the Ionian slab.

The final results provide the most accurate possible description of the tectonic structures shaping the Gulf and their activity within the broader framework of slab dynamics.

Backgrounds

Geodynamic setting

The geodynamic evolution of the Mediterranean region is driven by the ongoing convergence between the African and Eurasian plates at a rate of approximately 5 mm/yr (Billi et al. 2023; D'Agostino et al. 2008; Fig. 1b). In the former Western Mediterranean Sea, the plate margin was characterized by a subduction zone extending for 1,500 km from Iberia to the Liguria region (Faccenna et al. 2004; Fig. 1c). Since ~35 Ma, the hinge of this subduction zone has progressively retreated southeastward due to slab rollback, which has been accommodated by lithospheric tearing zones, ultimately reaching its present position beneath the Calabrian Arc (Faccenna et al. 2004, 2014; Jolivet et al. 2021; Rosenbaum and Lister 2004; Fig. 1b). Although the rate of slab rollback has varied over the past ~35 My (Gallen et al. 2023), it has never completely stopped; current geodetic data constrain it to 2–3 mm/yr (D'Agostino and Selvaggi 2004; D'Agostino et al. 2011; Palano et al. 2012).

During its retreat, the slab steepened, fragmented, and narrowed, reaching its current extent of less than 200 km between northeastern Sicily and southern Calabria, with an estimated dip of approximately ~70° and a depth of ~500 km, as evidenced by seismological data (Maesano et al. 2017; Neri et al. 2009; Scarfì et al. 2018; Selvaggi and Chiarabba 1995; Fig. 1b).

The present geodynamic setting results from a 1–0.7 Ma reorganization of the convergent margin, when the Sicilian and Apennines thrusts became mostly inactive, a compressional belt formed at the rear of the Sicilian orogenic wedge in the southern Tyrrhenian Sea, and a diffuse dextral transfer zone developed from eastern Sicily to the Western Ionian Sea to accommodate deformation along the last remnants of the WMSZ subducting beneath Calabria (Billi et al. 2007; Goes et al. 2004; Fig. 1b). The wide (~150 km) dextral

shear zone separates distinct upper plate tectonic regimes: a compressional belt north of the Sicilian coast and an extensional domain at the rear of the Calabrian Arc (Palano et al. 2012; Polonia et al. 2016; Fig. 1b).

This shear zone encompasses several crustal strike-slip fault systems:

- the Ionian Fault System (IFS; Polonia et al. 2016);
- the Alfeo-Etna Fault System (AEFS; Gutscher et al. 2016; Polonia et al. 2016);
- the Cefalù-Etna Fault System (CEFS; Barreca et al. 2016);
- the Capo Peloro Fault (Doglioni et al. 2012; Sgroi et al. 2025);
- the Scicli-Ragusa Fault System (Catalano et al. 2008);
- the Aeolian-Tindari-Letojanni Fault System (Billi et al. 2006; Ghisetti 1979; Lanzafame and Bousquet 1997; Palano et al. 2012, 2015).

Although the slab tearing results in a broad deformation zone in the upper plate, among these structures, the ATLFS is considered the most recent surface expression of the STEP fault at the southern edge of the subducting slab (Barreca et al. 2019; Palano et al. 2015; Scarfì et al. 2018).

This geodynamic reorganization coincides with the start of the rapid uplift in the Calabrian Arc and the onset of tholeiitic magma eruptions that led to the formation of Mount Etna (Casetta et al. 2020; Westaway 1993). Indeed, the subduction complex and lower plate geometry have strongly influenced volcanic activity in the region, including the southernmost Aeolian Islands, aligned along the northern portion of the ATLFS (Fig. 1a, b) (Peccerillo et al. 2013).

Similarly, Mount Etna location is thought to be linked to slab tearing, where differential rollback of the lower plate has produced either a slab window (Doglioni et al. 2001) or a complete discontinuity (Gvirtzman and Nur 1999). These structures may act as preferential pathways for asthenospheric upwelling material near the slab edge, as indicated by geochemical signatures analyses in erupted magmas. Such processes are considered potential drivers of Etna's volcanic evolution, controlled by decompression melting (Faccenna et al. 2011).

Asthenospheric upwelling, also inferred from GNSS data inversions (Palano et al. 2017), has been proposed as a contributing factor to the regional uplift of the Calabrian Arc, which has occurred at a rate of 0.8–1 mm/yr over the past ~ 1 My (Faccenna et al. 2011; Gvirtzman and Nur 1999; Westaway 1993).

This regional uplift, likely caused by dynamic topographic effects, is further modified by transtensional fault systems that cross the Calabrian Arc and the Sicilian Mountain range. These structures locally induce subsiding tectonic depressions, such as the Strait of Messina (Faccenna et al. 2011).

Geological setting

The study area lies on the structurally highest and innermost portion of the Sicilian Fold and Thrust Belt (SFTB), where the Calabrian-Peloritani terranes override the accretionary prism composed of stratigraphic successions from the Alpine Tethys and the African continental margin (Henriquet et al. 2020; and references therein), along the so-called Peloritani Sole Thrust (Catalano et al. 2018; Fig. 1a).

The Calabrian-Peloritani terranes (Fig. 1a) consist of crystalline units of the Variscan basement and a Meso-Cenozoic sedimentary nappe, locally covered by syntectonic deposits including the Oligocene flysch of Capo d'Orlando and Cretaceous mudstones of the Antisicilide formations (Cirrincione et al. 2015).

During the middle-late Miocene, a significant shift in the tectonic regime led to subsidence in the innermost part of the Peloritani range (Lentini et al. 1995), a transition driven by the onset of NW-SE directed tectonic stretching associated with the opening of the southern Tyrrhenian Sea. This results in the late Miocene–Quaternary succession unconformably overlying older deposits (Lentini et al. 1995; Fig. 1a).

This tectonic evolution, linked to the opening of the southern Tyrrhenian Sea, propagated throughout the innermost part of the SFTB and triggered subsidence in the Peri-Tyrrhenian basins of Gioia and Cefalù since Tortonian time (Fabbri et al. 1981). While extension in the Gioia Basin continues to present-day, the Cefalù Basin has experienced tectonic inversions (Billi et al. 2011, 2023; Goes et al. 2004).

The transition zone between those tectonic regimes is centered in the Gulf of Patti, along the Aeolian-Tindari-Letojanni Fault System (ATLFS), an active dextral strike-slip lithospheric fault system with a lateral displacement of 6–7 km (Ghisetti et al. 1979) currently accommodating a differential deformation of about 3.6 mm/yr (Palano et al. 2012).

Despite various studies, the geometry, activity, and accurate location of individual faults within this complex deformation belt remain poorly constrained, particularly in its southern sector. Dip-slip and strike-slip faults mapped near the Ionian coast have been interpreted as the southernmost expression of the ATLFS (Ghisetti 1979), with some authors proposing a connection between these faults and tectonic structures in the Ionian Sea (Barreca et al. 2019; Lanzafame and Bousquet 1997; Palano et al. 2015). However, this connection has been questioned by other studies, which place the southern termination of the ATLFS approximately 6–7 km southeast of Novara di Sicilia (Billi et al. 2006).

North of Novara di Sicilia (NS, Fig. 1a), the ATLFS is part of the Nebrodi-Peloritani Transition Zone, a broader network of NW-SE and WNW-ESE dextral strike-slip structures (Pavano et al. 2015). These structures have controlled the formation of several ridges, such as Capo Calavà and Capo Tindari, as well as tectonic depressions, including the Patti and Castroreale-Barcellona basins (Nigro and Renda 2005; Fig. 1a). The Castroreale-Barcellona basin, in particular, is a triangular-shaped structural depression bounded to the west by a set of NW-SE/NNW-SSE transtensive faults associated with the principal deformation zone of the ATLFS. A second set of extensional faults, oriented NNE-SSW, has been mapped within the basin and along its eastern border (Billi et al. 2006; De Guidi et al. 2013; Cultrera et al. 2017a; Fig. 1a).

The Gulf of Patti has recently been considered the offshore counterpart of the Castroreale-Barcellona tectonic depression, which formed through extensional tectonics along the offshore prolongation of the ATLFS (Colantoni et al. 2001; Cultrera et al. 2017a; Cuppari et al. 1999; Fig. 2). Although a dense network of extensional faults has been identified within the Gulf, the origin of the central NW-SE oriented morphological high, known as the "Patti Ridge", remains poorly constrained. This structure has been interpreted as formed by geometry variations along the ATLFS (Fig. 2a; Cuppari et al. 1999), or as an anticline produced by compressive to transpressive tectonics active since the middle Pleistocene (Fig. 2c; Argnani et al. 2007); this latter interpretation also explains the uplift observed at Capo Milazzo promontory, where Argnani et al. (2007) described a tectonic anticline (Fig. 2c).

A more recent interpretation suggests the presence of a pull-apart basin formed by a releasing stepover between two segments of the ATLFS, i.e., the Tindari-Novara Fault Zone (TNFZ) and the Vulcano-Milazzo Fault Zone (VMFZ) (Cultrera et al. 2017a; Fig. 2d).

Methods

Marine geophysical data

The morphobathymetric map used in this study was derived from data collected using a SIMRAD 710 multibeam system aboard the R/V Minerva Uno of the Italian CNR during the GEOHAZIS2015 cruise. High-resolution CHIRP sonar sections (maximum penetration of about 0.100 s TWT) were obtained using a Teledyne-Benthos system equipped with 15 transducers during the same cruise (Fig. 3).

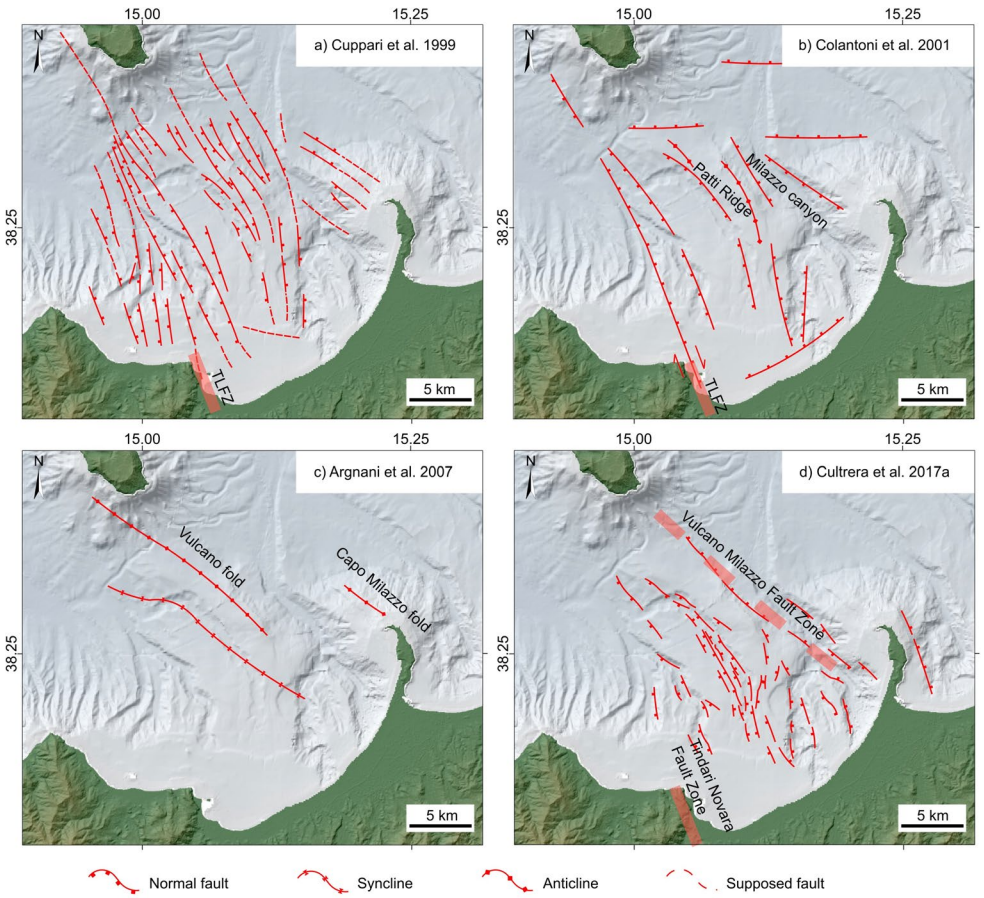

Fig. 2 Different structural maps describing the Gulf of Patti, drawn over a morphobathymetric map compiled using data from EMODnet (http://www.emodnet-bathymetry.eu): (**a**) the Gulf is crossed by the prolongation of the Tindari-Letojanni Fault Zone (TLFZ) resulting in a NNW-SSE deformation zone, consisting of recent extensional faults with an inferred right lateral component (Cuppari et al. 1999); (**b**) the main faults are NNW-SSE oriented and bound the Patti Ridge and the Milazzo Canyon, showing evidence of recent extensional tectonics (Colantoni et al. 2001); (**c**) contractional deformation has been active in the Gulf of Patti since middle Pleistocene, resulting in the formation of two broadly overlapping anticlines, the Vulcano (corresponding to the "Patti ridge") and Capo Milazzo folds (Argnani et al. 2007); (**d**) two major NW-SE trending right-lateral transtensional fault zones, namely the Vulcano-Milazzo Fault Zone and the Tindari-Novara Fault Zone, generate a releasing stepover (Cultrera et al. 2017a)

The primary dataset consists of a dense grid of Multichannel Seismic (MCS) profiles, with a penetration of around 1.5 s TWT, acquired during the SEADRONE (2019) cruise aboard the R/V Dallaporta of the Italian CNR (Fig. 3). The seismic source used was a Bubble Gun, a low-frequency boomer system developed by HMS (Falmouth, USA), while the receiver was a 16-channel Geometrics GeoEel streamer. MCS data were processed using RadExpro software to generate time-migrated sections. Additionally, the newly acquired seismic reflection data were integrated with three single-channel seismic profiles (maximum penetration of about 2 s TWT) collected in the 1970 s aboard the R/V Bannock of the Italian CNR during the BS78-II cruise, using a Sparker-30 kJ system (Fig. 3).

Data interpretation and analysis were performed using the open-source software SeisPrho 3.0 (Gasperini and Stanghellini 2009). Pseudo-3D time-slice images were generated following the procedure described by Gasperini et al. (2021). MCS profiles underwent a flattening process, whereby they were time-shifted to align with a horizontal reference level (0 ms) and sampled at different Two-Way Traveltime (TWT) windows using the corresponding SeisPrho function. The resulting time slices were integrated to compute the Cumulative Amplitude Index (CAI), which provides an estimate of seismic facies characteristics and the lateral coherence of reflectors within the selected TWT-frame (Gasperini et al. 2021).

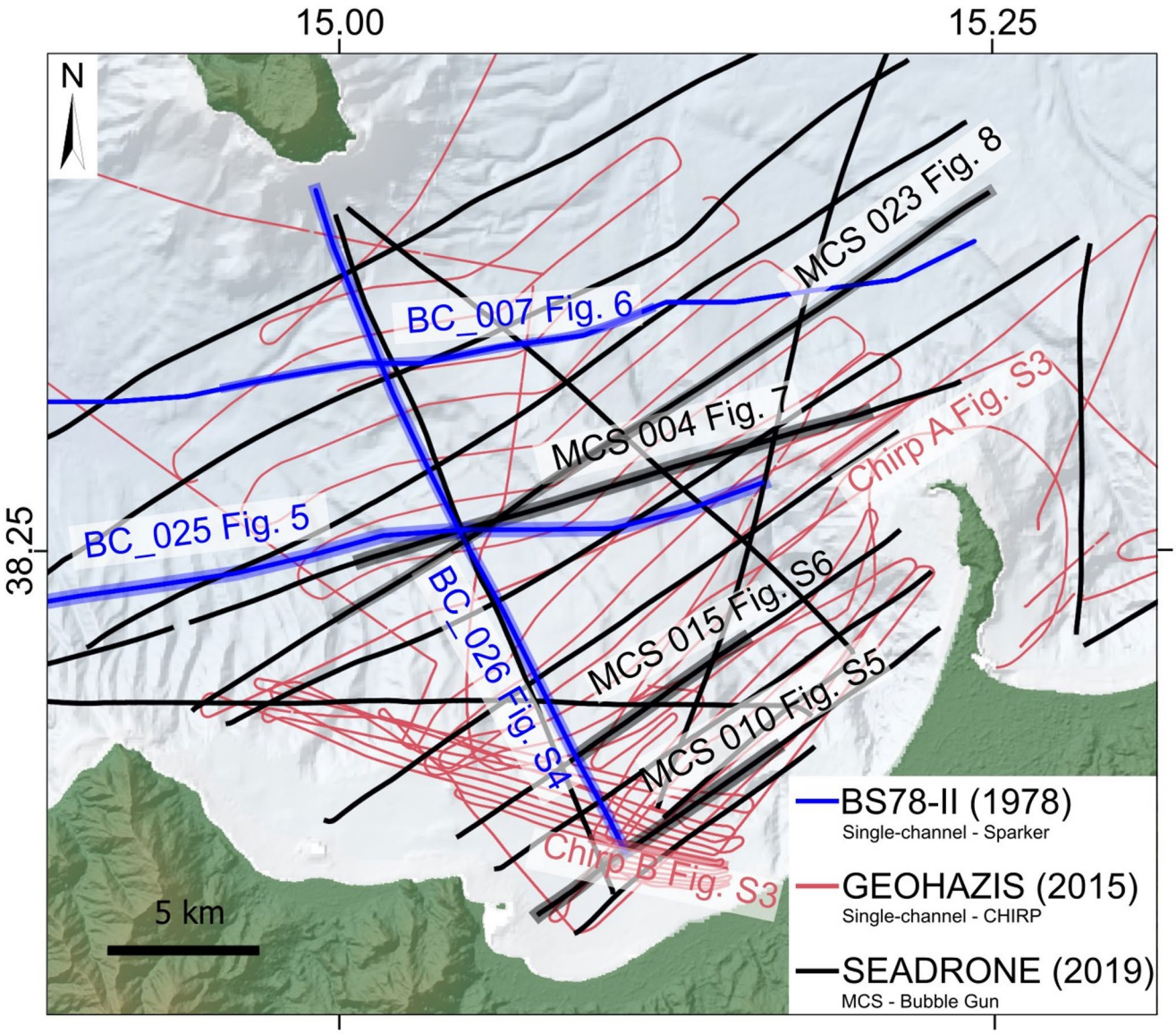

Fig. 3 Network of multi-resolution seismic reflection data used in this work. Thicker lines represent seismic profiles displayed in this work

Seismological datasets

A new earthquake catalog for crustal and sub-crustal events (up to 100 km depth) was compiled by collecting travel times of events, occurred from January 2000 to August 2021, extracted from the Italian Seismic Bulletin (Working Group 2007) and the "Catalogo della Sismicità Italiana" (CSI; Castello et al. 2006) for land stations (Fig. S1). The selected travel times from land stations were then integrated with those handpicked for the events recorded, between December 2000 and May 2001, on the Ocean Bottom Seismometers (OBSs) network deployed during the TYrrhenian Deep-sea Experiment (Dahm et al. 2002; Sgroi et al. 2006; Fig. S1).

This integrated land-sea dataset (https://doi.org/10.13127/styrr_eq3d/2000-2021), consisting of more than 8,000 earthquakes, was relocated using the tomoDDPS algorithm (Zhang et al. 2009) and a regional 3D velocity model available for the area (Scarfì et al. 2018).

To obtain more information about the surrounding and deeper regions, we extracted the locations of earthquakes that occurred within the same time interval of the integrated land-sea dataset, at depths between 100 and more than 600 km, as well as the events that occurred in proximity to the Messina Straits (MES) from the dataset recently published for the MES region (Sgroi et al. 2025).

This combined catalog consists of more than 13,000 earthquakes ($0.6 \leq$Md-Ml-Mw≥ 5.8) located in the southern Tyrrhenian – North Sicily area, with depths ranging from the surface down to about 600 km.

We computed the focal mechanisms by applying the FPFIT standard procedure (Reasenberg and Oppenheimer 1985) selecting earthquakes that occurred in southern Tyrrhenian and northern Sicily at depths of up to 100 km. Only earthquakes with at least eight clearly identified polarities, and homogenously distributed over the focal sphere, are considered.

A total of 268 focal mechanisms of events located both offshore and onshore were computed (https://doi.org/10.13127/styrr_fm/2000-2021; Fig S2).

Approximately 60% of events have a number of polarities≥ 10 and about 67% of earthquakes do not show discrepant polarities. The quality of each solution was assessed based on polarity misfit and the uncertainty ranges of strike, dip, and rake values. In this dataset, 131 focal solutions have best quality (2.0) and 137 focal mechanisms have intermedium quality (1.0), while we excluded the events with the worst quality (0.0). This new computed dataset of focal mechanism shows similarities with the focal mechanisms previously published by other authors (e.g., Neri et al. 2005; Scarfì et al. 2016).

The focal mechanisms showing the higher quality were used to determine the principal stress axes and the parameter (shape ratio) $R = (\sigma 2\text{-}\sigma 1)/(\sigma 3\text{-}\sigma 1)$, a dimensionless coefficient that represents the shape of the stress tensor. The method, which exploit a standard numerical technique (Gephart 1990; Gephart and Forsyth 1984), identifies the best stress tensor model matching the considered focal mechanisms.

Results

Seafloor morphology

The Gulf of Patti is shaped by various geological processes, including landslides, channelized flows, and faulting, resulting in an irregular seafloor morphology (Fig. 4).

The continental shelf in this region is relatively narrow, with its minimum width towards the east, where retrogressive erosion driven by canyons reaches close to the coastline (Fig. 4). The shelf shows its maximum extension (~5 km) in the central sector, where multiple gullies actively erode the shelf break. North of Capo Tindari, the shelf break is irregular and marked by bedrock outcrops along the Tindari Ridge (Fig. 4).

The center of the Gulf is occupied by the so-called "Patti Ridge" (Fig. 4). The topographic high, roughly oriented NW-SE, represents the sill (~420 m b.s.l.) between the Gioia and Cefalù basins (Fig. 4). To the west, an incised canyon called "Patti Valley" extends in the same direction and abruptly changes its course just south of the Vulcano Island (Fig. 4).

Fault-controlled canyons bound the Patti Ridge (Fig. 4). Their upper courses are approximately oriented N-S, and bend toward NW-SE close to the basin center, together with all the main morphological elements. The straight thalwegs suggest a control exerted by active faults, but tectonic deformation appears partially overprinted by erosional and gravitational instability processes. Similarly, we observe a rotation of the canyon courses from NNE-SSW to N-S and NW-SE, west of Capo Tindari.

Several gravitational failures have been recognized in the steepest sectors of the study area, along the canyon walls, the flanks of the ridge, and along the continental shelf, where creep processes create an irregular morphology (Figs. 4, S3).

Multibeam data only partially cover the northern sector of the study area. Nevertheless, we highlight the presence of two canyons roughly oriented ENE-WSW that branch from the Patti Sill (Fig. 4). Furthermore, close to Vulcano island, the volcanic outcrops, gullies, and canyons contribute to a rugged morphology.

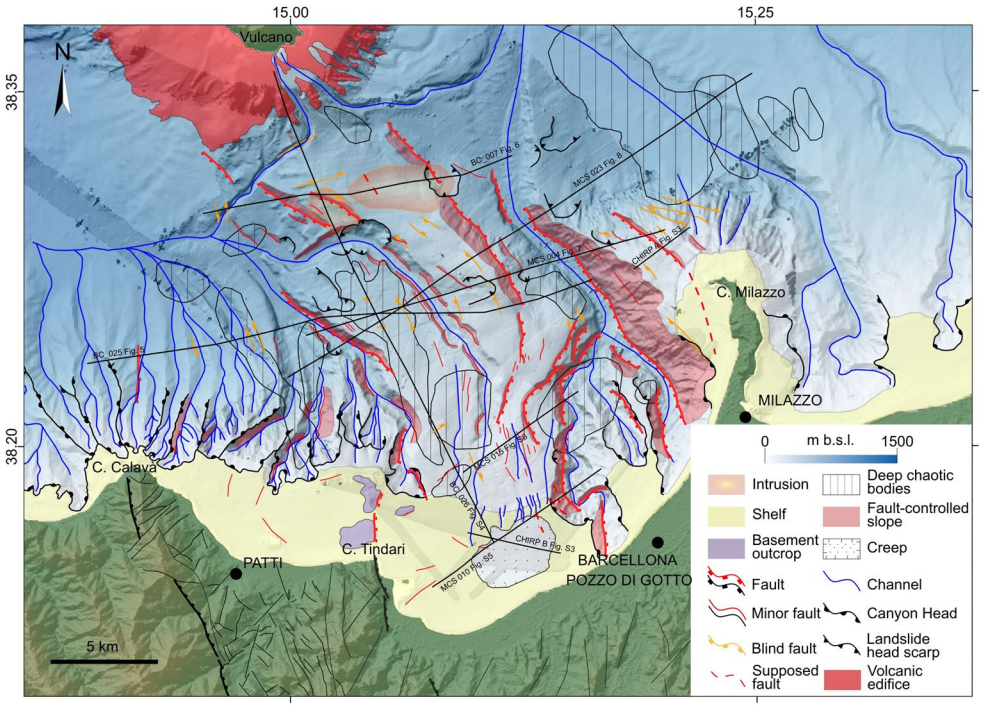

Fig. 4 Morphostructural map of the study area. The bathymetric map is compiled using our new surveys and data recovered from EMODnet repository (http://www.emodnet-bathymetry.eu). Location of volcanic edifice, shelf breaks, and canyon heads are taken from the MaGIC project repository (sheet 17 Milazzo, and 18 Capo d'Orlando; Gamberi et al. 2024). Tectonic features of the onshore region between Capo Tindari and Capo Milazzo are based on Billi et al. (2006), Cultrera et al. (2017a). Faults of the onshore area between Capo Calavà and Capo Tindari are based on the Geologic Map of Italy (sheet 599 and 587–600) (Servizio Geologico d'Italia 2011, 2013)

Seismic reflection data

The analyzed dataset consists of a dense grid of seismic profiles collected using different seismic sources characterized by varying penetrations (see the Methods section). These data allowed us to investigate the sub-bottom structure of the Gulf at various depths, albeit with differing resolutions. However, no boreholes are available in the area to calibrate seismostratigraphic observations.

We based our stratigraphic framework on correlating data available from surrounding areas and published studies. These include descriptions of seismic facies and sedimentary samples recovered from the canyons (Fabbri et al. 1981; Selli and Fabbri 1971), as well as subsequent studies carried out by different working groups (Argnani et al. 2007; Colantoni et al. 2001; Cuppari et al. 1999).

In the regional 30 kJ sparker seismic reflection profiles, we identified a major discontinuity correlated with the base of the Plio-Quaternary (PQ) succession, consistent with previous studies.

Below this unconformity, we named Unit-B a seismostratigraphic unit characterized by high-amplitude, corrugated, and fairly continuous reflectors (Fig. 5). This unit correspond to the Unit-B2, interpreted as Messinian marginal facies deposit by Fabbri et al. (1981), and may also correspond to the bedded unit (BU), following the classification of the Messinian salinity crisis seismic markers proposed by Lofi et al. (2011).

The PQ deposits, grouped in our Unit-A, can be divided into two sub-units, -A1 (above) and -A2 (below), separated by a regional infra-Pliocene unconformity (Fig. 5). This surface corresponds to the "Unconformity X" of Fabbri et al. (1981) and has been recognized by several authors across other peri-Tyrrhenian basins, such as the Sardinia basin (Lymer et al. 2018).

Unit-A2 is locally acoustically transparent or composed of low-amplitude reflectors, and it maintains a nearly constant thickness. Samples dredged from this unit in the nearby Stromboli Canyon show lithological and paleontological features compatible with the marly "Trubi" Formation (Selli and Fabbri 1971). Unit A1 displays high-amplitude continuous reflectors, probably representing a turbidite sequence, that thins over the topographic highs and thickens towards the west of the Gulf (Fig. 5). A local uniformity (orange dotted line in Fig. 5) marks a change of the acoustic facies between the lower and upper part of the Unit-A1. The lower and older portion of the unit is marked by low amplitude and locally more irregular reflectors relative to the upper portion, that appears slightly thicker in the central part of the Gulf (Fig. 5).

Profiles BC-07 and BC-26 (Figs. 6, S4) show two basement highs rising through the sedimentary succession in correspondence to extensional deformations just south of Volcano island. They are marked by acoustically blind facies delimited by strong reflections at their top, suggesting the presence of magmatic intrusions.

The MCS boomer profiles (Fig. 7) show higher resolutions but more limited penetration. Indeed, they do not always allow for imaging the top of Unit-B, or recognizing the infra-Pliocene unconformity, i.e., the discontinuity

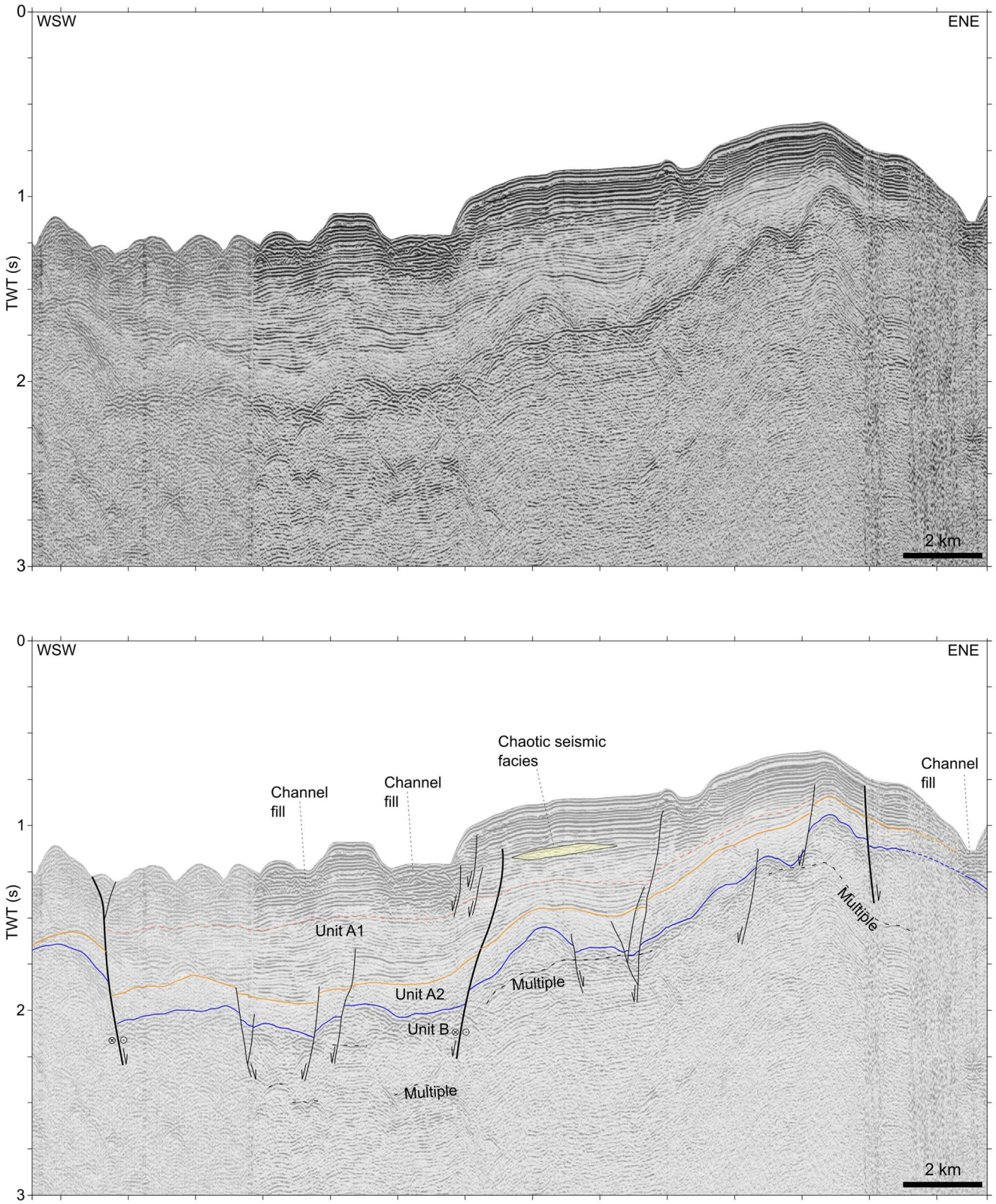

Fig. 5 Seismic profile BC_025 and its interpreted line-drawing (location in Fig. 3). The profile illustrates the general architecture of the Gulf of Patti, showing a sedimentary succession that thickens westward and is bounded by major faults delimiting tilted blocks. Blue line: base of the PQ succession; light orange line: infra-Pliocene regional unconformity; orange dotted line: local unconformity.Yellow polygons: Chaotic seismic facies. The strike-slip component of the faults is inferred combining seismo-stratigraphic and seismological observations

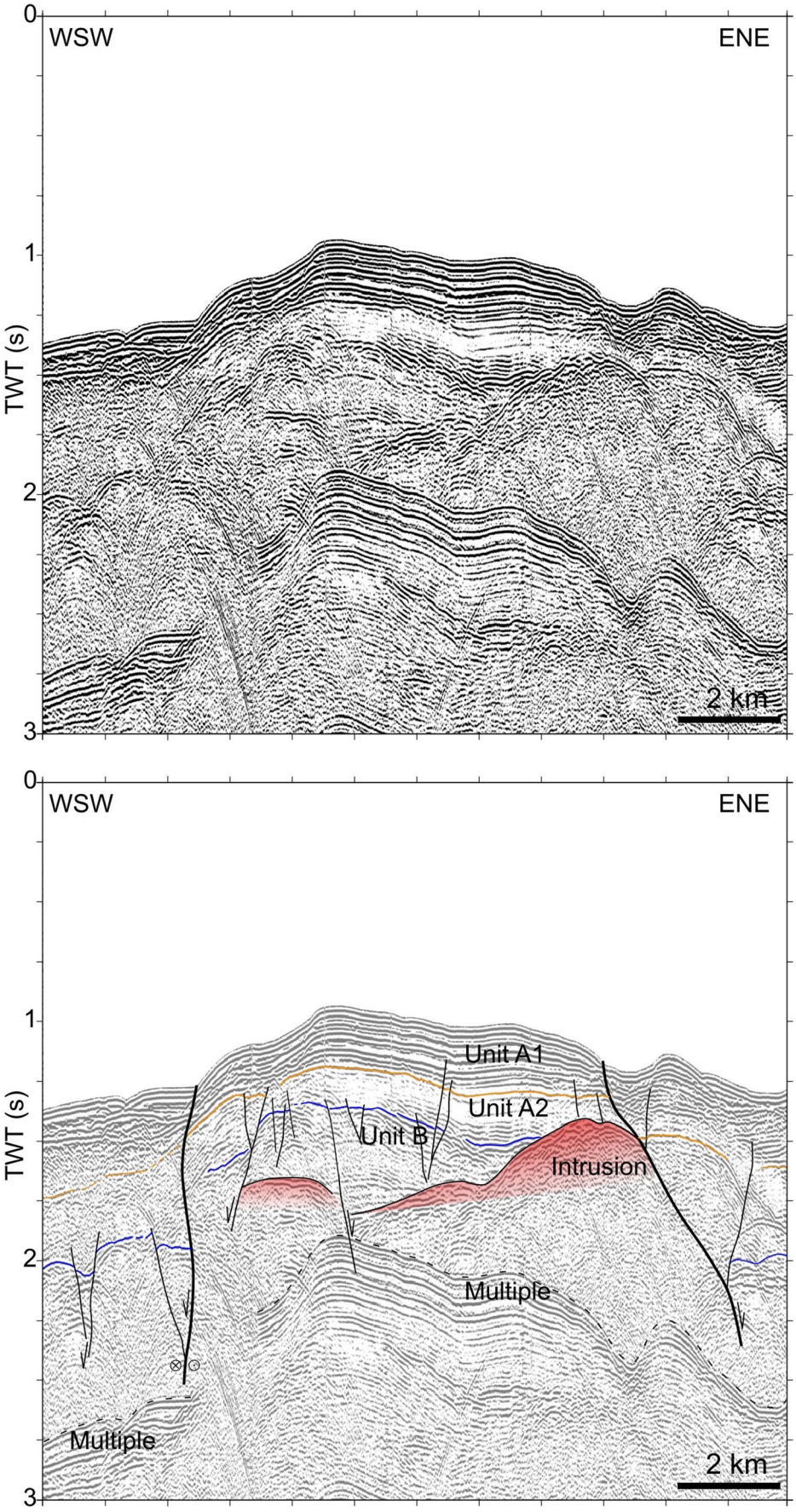

Fig. 6 Seismic profile BC_007 and its interpreted line-drawing (location in Fig. 3). Two bedrock highs, probably intrusions bounded by faults, are visible. To the west, a major transtensive fault cuts the sedimentary succession up to the seafloor. Blue line: base of the PQ succession; light orange line: infra-Pliocene regional unconformity; red polygons: magmatic intrusions. The strike-slip component of the faults is inferred combining seismostratigraphic and seismological observations

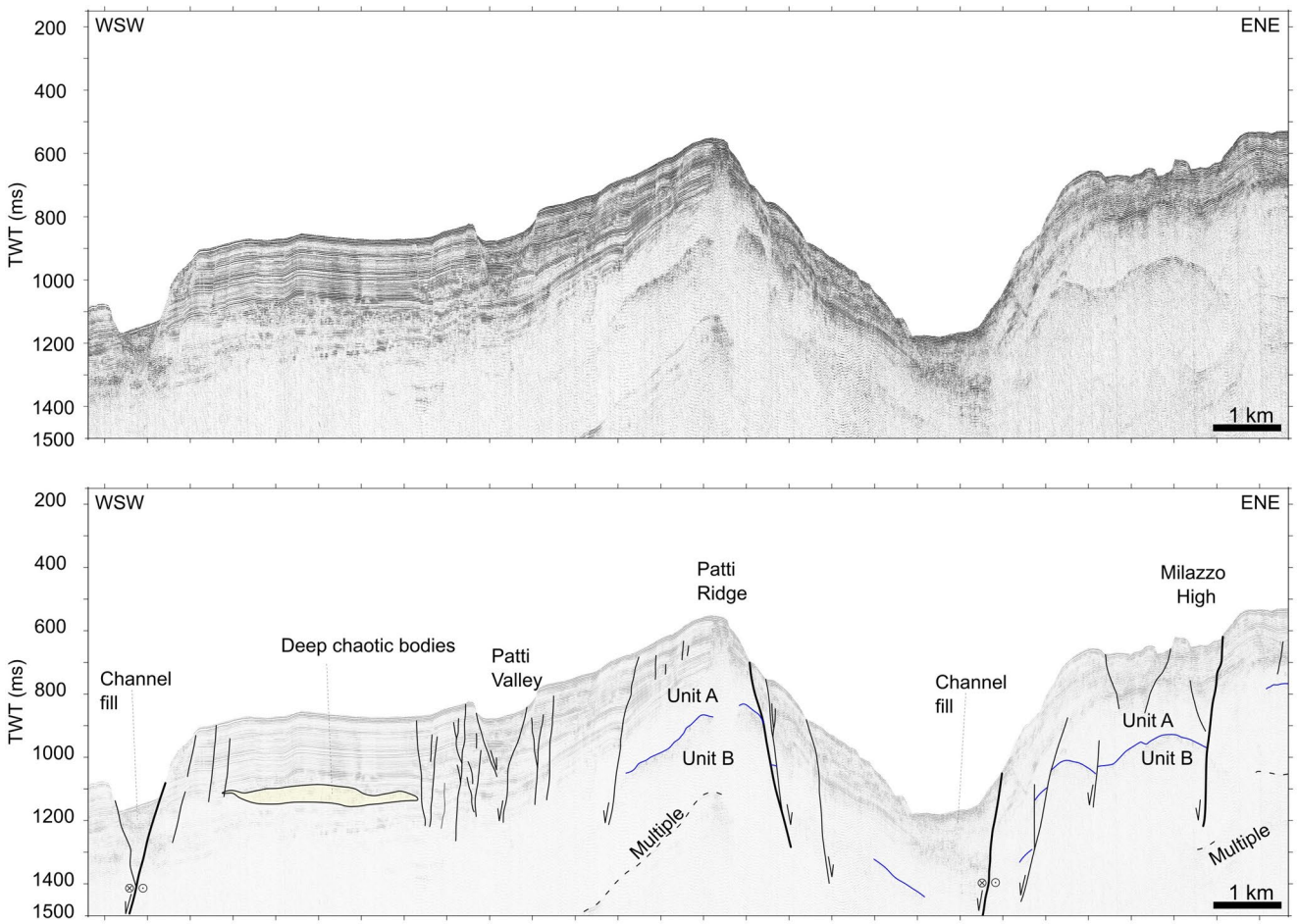

Fig. 7 Seismic profile MCS_004 and its interpreted line-drawing (location in Fig. 3). Pervasive deformations affect the sediments, while major faults bound the Patti Ridge and control the direction of incised canyons. Blue line: base of the PQ succession; yellow polygons: chaotic seismic facies. The strike-slip component of the faults is inferred combining seismo-stratigraphic and seismological observations

between Unit-A1 and Unit-A2. However, the higher resolution enables a more accurate analysis of the internal architectures of the Unit-A1 and continental shelf deposits, including Holocene base, as well as an older unconformity delimiting a progradation wedge probably older than the Tyrrhenian (Fig. S5).

In the uppermost units, we identified the diffuse presence of slump deposits, recognized by lenticular shapes and massive to chaotic patterns (Fig. 7).

The Gulf of Patti hosts active tectonic deformations of different nature and extents, primarily represented by subvertical fault planes. A major fault north of Capo Calavà, imaged in profile BC_025, affects the entire sedimentary succession and bounds a relatively wide (about 20 km) asymmetric basin, with clear evidence of tilting towards the WSW (Fig. 5). Other faults bound the Patti and Capo Milazzo highs, controlling the formation of submarine canyons (Fig. 7).

Overall, the basin architecture is dominated by a set of NW-SE oriented faults with subvertical or high-angle planes that accommodate extensional dip-slip deformation, as shown by reflector offsets in the seismic profiles (Figs. 4 and 7). These faults likely also accommodate a significant strike-slip component, as indicated by seismological data (see next sections). The only exceptions are several NE-SW extensional faults recognized in the BC profiles, probably related to volcanic accretion and deformation of the basement (Fig. 4).

The fault pattern becomes more complex to the south, between Capo Calavà and Capo Tindari and between Capo Tindari and Capo Milazzo, where faults trend N-S to NE-SW (Fig. 4).

In the central part of the Gulf, along the Patti Valley and Patti Ridge, we observe widespread deformation accommodated by secondary structures with minor slip. These minor faults may represent damage zones along the main ATLFS segments, such as the fault bounding the Patti Ridge. Bends in these main transcurrent faults can produce negative flower structures, as in the profile MCS_015 at the southern

termination of the fault bounding the Patti Ridge (Figs. 4, S6).

Pseudo-3D subseafloor images

Two-Way Traveltime (TWT) slices at different levels were obtained using the pseudo-3D seismic technique described in the methods section (Fig. S7). Each slice shows the horizontal distribution of the Cumulative Amplitude Index (CAI) at a given level, allowing visualization of lateral changes in seismic facies related to differences in reflector patterns. Such variations can be interpreted as deformation or departure from a planar parallel layering. This information helps map tectonic and gravitational structures when cross-checked with 2D seismic sections.

Observed lateral changes in the acoustic facies are mainly oriented NW-SE, aligning with the main canyon axes and other morphological features, including fault patterns. A sharp lateral contrast in acoustic facies often reflects dislocation across a fault, as seen at the boundary of the unit with relatively low CAI, centered below the Patti High (Fig. 8d).

Units with lower CAI show higher-continuity reflectors, such as the superficial turbiditic succession. Higher CAI corresponds to lower-continuity, more chaotic or discontinuous bodies, which in our case study display very high amplitude reflections. In the shallower TWT slices, higher CAI values correspond to submarine-channel fill and gravitational deposits on canyon slopes (Fig. 8c).

High CAI patterns, not always oriented along the main tectonic trend, are also visible far from the submarine canyons and locally at greater depths. These patterns represent the chaotic bodies mapped on the seismic profiles. By combining TWT slices and seismic profiles, we were able to map these bodies interpreted as gravitational instability deposits (Fig. 4).

The pseudo-3D representation of the seismic data suggests that many exogenous and endogenous geological processes control the shape of the Gulf of Patti at different scales.

Relationship between faults and seismicity

Figure 9 illustrates the distribution of earthquakes, occurred between January 2000 and August 2021, at the southwestern edge of the Calabrian Arc. The Gulf of Patti and the onshore extension of the tectonic depression are among the most seismically active sectors of the upper plate. A shallow seismicity zone, extending to depths of 15 to 17 km within the lithosphere and elongated in the NNW-SSE direction, crosses the Gulf and aligns with the central Aeolian Islands. This shallow seismogenic corridor overlaps a region centered on the Gulf that lacks deeper seismicity.

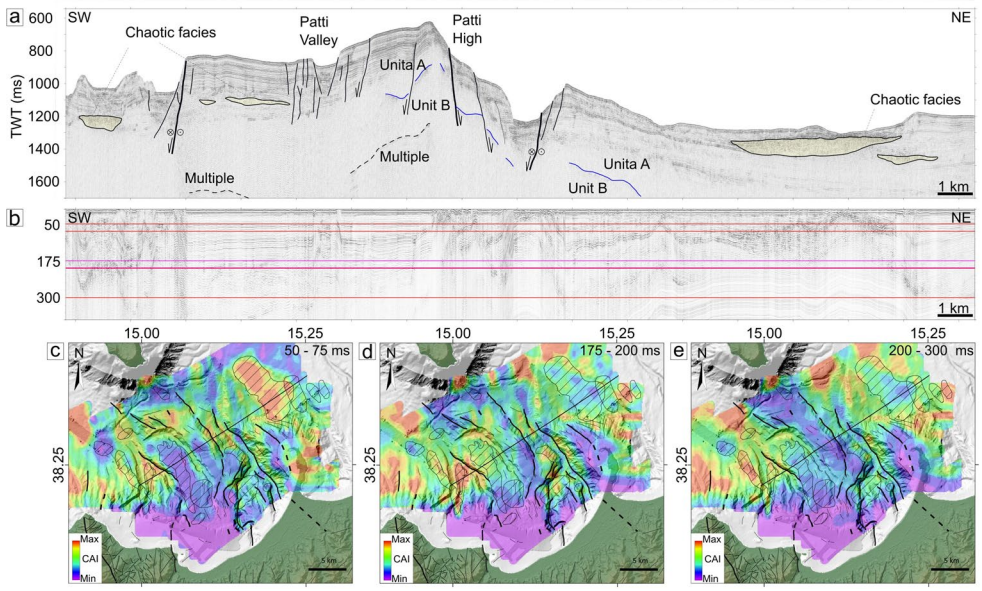

Fig. 8 (**a**) Seismic profile MCS_023 (position in maps below) with main structural and depositional elements indicated. Diffuse tectonic deformation affects the Patti Ridge and the bounding canyons. Chaotic facies, possibly related to mass-transport deposits or channel infill, are recognized in the shallower seismostratigraphic unit and marked with light yellow polygons. Blue line: base of the PQ succession. (**b**) flattened version of profile MCS_023. Red and purple lines indicate time-slice levels of the colour maps below; (**c**), (**d**), (**e**) Cumulative Amplitude Index (CAI) maps for different TWT slices. Areas affected by tectonic or gravity instability, as well as hard bedrock outcrops, are characterized by lower coherence of the CAI within the map. Comparing CAI patterns observed in TWT slices with seismic reflection lines extends the 2D interpretation to a 3D

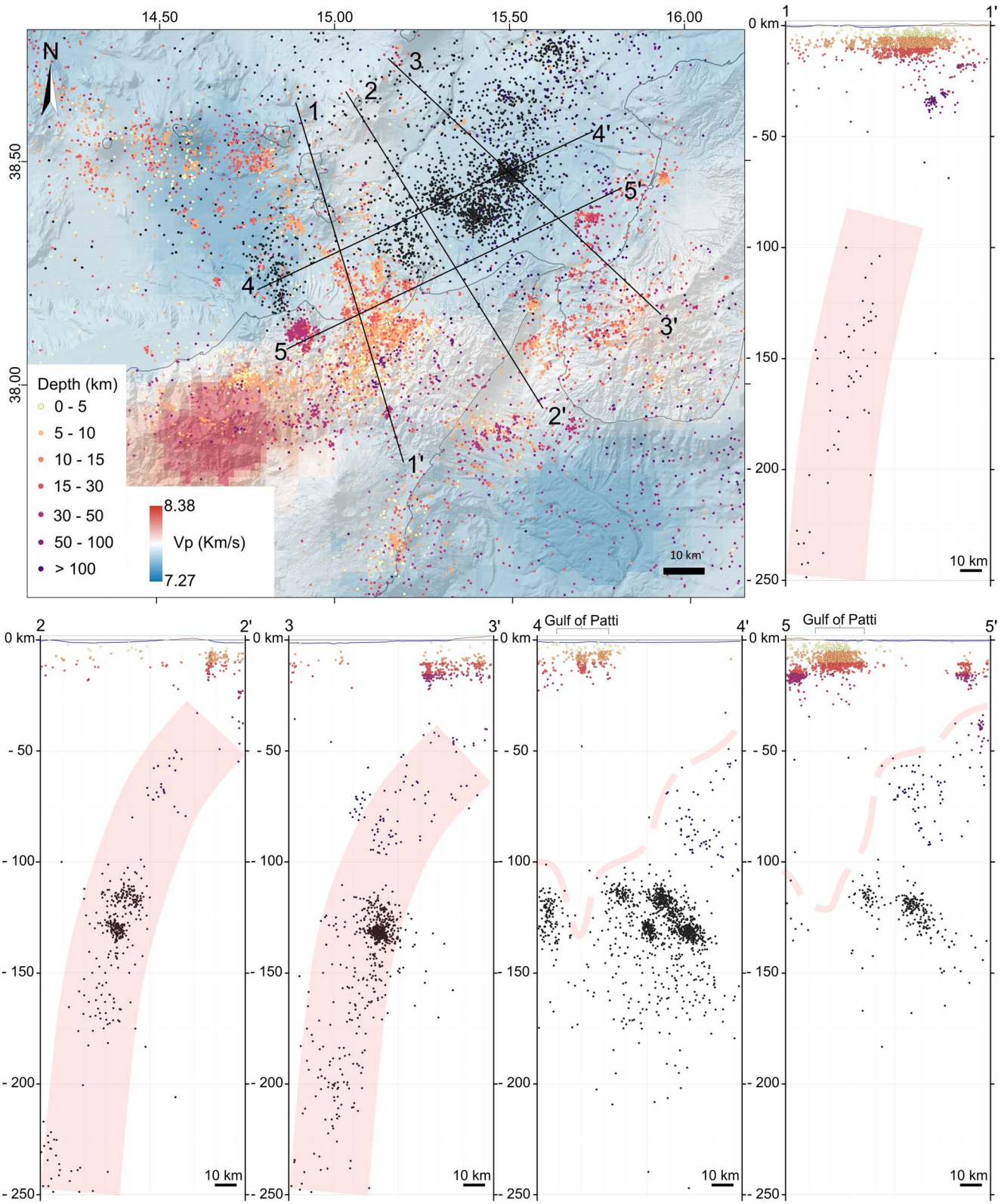

Fig. 9 Seismicity map and sections of the southwestern edge of the Calabrian arc. The map is plotted over the Vp model at 40 km depth (from Scarfì et al. 2016). In the five ~ 92 km long sections, hypocentres are projected within ± 8 km of the traces (1–5) shown in the map. Light red bands mark the average depth of deep-seated seismicity that outline the top of the Ionian slab in Sects. 1–3. In Sects. 4 and 5, events below the dotted lines represent the deep-seated seismicity related to the slab or slab relicts

Furthermore, the shallow seismicity zone coincides with the boundary between two distinct crustal domains differentiated by seismic wave velocity (V_p): higher V_p to the northeast and lower V_p to the southwest, as indicated by the seismic velocity inversion model (Fig. 9; Scarfì et al. 2016).

Hypocenter projections suggest that the subducting slab has already broken off beneath the Gulf (Sects. 1–1', Fig. 9). Deep seismicity west of the Gulf may represent slab remnants (Sects. 4–4', Fig. 9), while the slab appears continuous in the eastern sections (Sects. 2–2' and Sects. 3–3', Fig. 9).

Projections nearly longitudinal to the slab show the highest density of shallow seismicity within the Gulf and the onshore tectonic depression, overlapping an area lacking deep seismicity. The edge of the still-continuous slab lies to the east of the gulf near Capo Milazzo Peninsula, whereas near Capo Peloro, there is a high concentration of deep earthquakes (Fig. 9).

Within the Gulf, the shallow seismogenic corridor aligned with the Central Aeolian Islands broadens and is largely confined between Capo Tindari and Capo Milazzo, an area highly deformed by numerous fault sets. This confirms that the deformation zone identified in the pseudo-3D model is seismically active.

Among the newly determined focal mechanisms (Fig. 10): most of them exhibit normal (127 events) and transtensive (61 events) kinematics, while only 18 solutions are characterized by compressive (7 events) or transpressive (11 events) kinematics. Additionally, the 28 strike-slip mechanisms and the 34 horizontal-vertical mechanisms account for 23% of the observed kinematics.

Focal solutions distribution shows that pure strike-slip movement dominates in the north (Fig. 10) with additional strike-slip events near Capo Milazzo. In contrast, extensional and transtensional kinematics prevail in the central part of the Gulf.

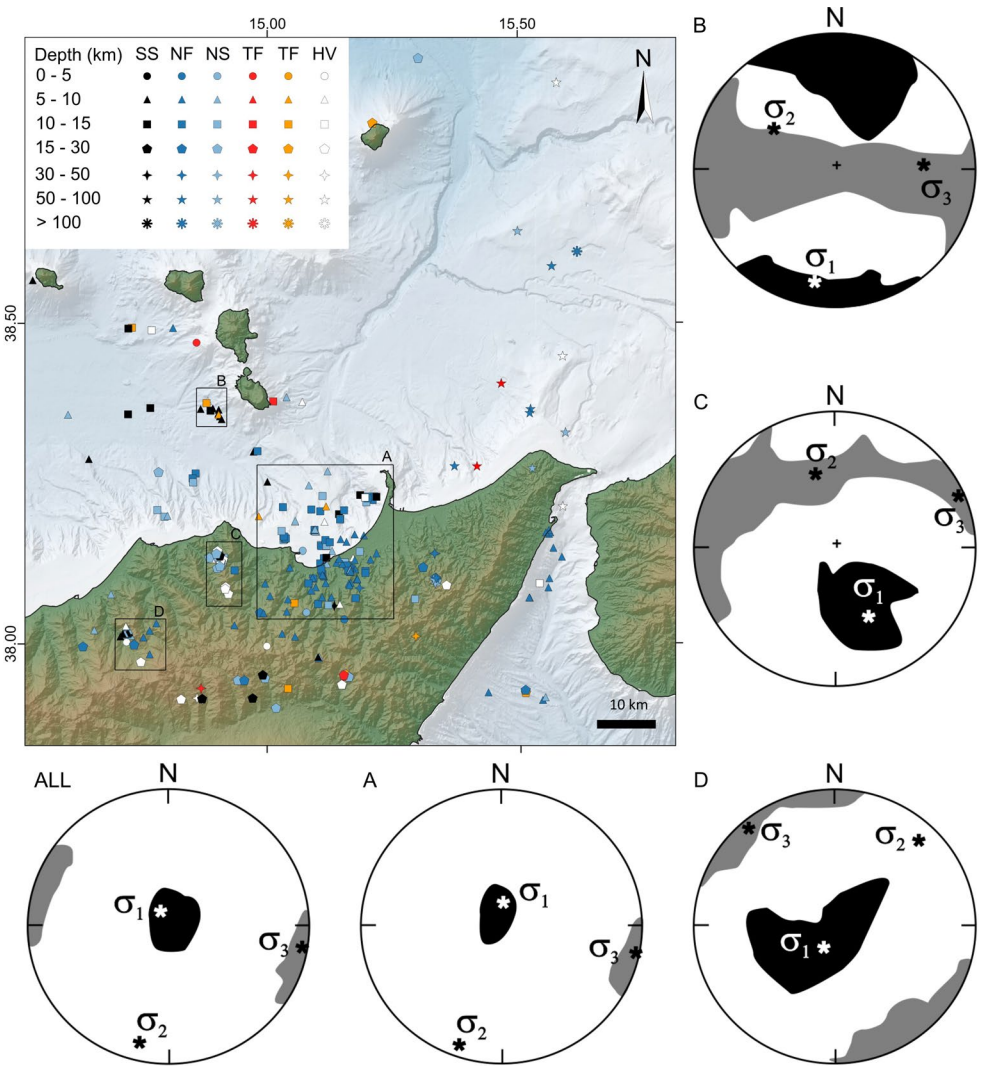

Fig. 10 Location map of focal solutions categorized according to the kinematic classification (Fröhlich 1992) and stress tensors from the focal mechanism inversions of the entire dataset (ALL) and the four sectors defined by black boxes on the map (**A**, **B**, **C**, **D**). Colour legend: NF = normal fault, NS = normal strike, SS = strike slip, TF = thrust fault, TS = thrust-strike, HV = horizontal-vertical

Stress inversion

The 268 focal mechanism events calculated in this work were inverted to compute the stress tensor of the study area. The stress tensor obtained by inverting the 268 focal mechanisms (Table 1) shows σ_1 and σ_3 oriented at 337° and 105°, respectively, with dips of 79° and 7°. However, the resulting misfit (F = 9,276°) indicates a large heterogeneity of the stress regime, following Gillard et al. (1996), Lu et al. (1997), and Wyss et al. (1992) who suggested that an F < 6° corresponds to a homogeneous stress regime, whereas an F > 9° represents a heterogeneous stress regime.

The inversion analysis was repeated, subdividing the dataset into different groups according to the location of the events and structural heterogeneities, resulting in four groups (Fig. 10; Table 1).

Group-A is the largest, and includes 120 events in the Gulf of Patti at a depth shallower than 15 km. The stress tensor resulting from inversion (F = 6.289; R = 0.5; σ_1 = N339°E dipping 82°; σ_2 = N198°E dipping 6° σ_3 = N107°E dipping 5°) is quite homogeneous, and exhibits very limited 95% confidence areas. The tectonic regime indicated by Group-A stress tensor is extensional, according to the World stress map stress regime categorization table (Zoback 1992).

Stress tensors compiled for the other three groups, located to the north (Group-B) and to the west (Group-C and Group-D), show different orientations of the stress axes compared to each other and to Group-A (Fig. 10; Table 1). This led us to distinguish different tectonic regimes: extensional for Group-D, transtensional for Group-C, and strike-slip for Group-B. The misfit of these latter groups is generally very low, indicating high homogeneity, although based on a relatively small number of events, which result in large confidence areas for the orientation of the stress axes.

Discussion

Analysis of multiscale seismic reflection profiles, morphobathymetric data, and seismological observations has allowed us to refine the tectonic model of the Gulf of Patti (Fig. 11). This integrated approach allowed mapping of active tectonic features as well as erosional and gravitational morphologies shaping the area.

Our geological model raises key questions about the link between surface morphologies and crustal deformation at the edge of the Calabrian slab. Specifically, we address whether and how seafloor morphologies reflect the underlying tectonic processes and how morphological highs occur within a region largely characterized by transtension along the ATLFS.

Building a tectonic model

Morphostructural and TWT-slice maps of the Gulf of Patti show that the irregular seafloor and subseafloor morphology is the result of interacting geological processes at different scales, tectonic deformation and gravitational failures. These represent the shallow expression of a complex tectonic pattern at the Calabrian slab edge. Although sediment supply, erosion, and flooding contribute, tectonic deformation is the main driving process generating the steep topographic gradients. Moreover, seismic shaking from frequent earthquakes likely triggers much of the observed gravitational instability.

The Gulf is crossed by a principal NNW-SSE oriented deformation zone, previously described in the literature (Fig. 2; Argnani et al. 2007; Colantoni et al. 2001; Cultrera et al. 2017a; Cuppari et al. 1999). Most authors interpret this zone as active extensional to transtensional (Fig. 2a, b, d). Argnani et al. 2007 instead interpret the two morphological high in the gulf as anticlines (Fig. 2c), and infer compressive/transpressive tectonics active since the middle Pleistocene.

Despite the complex morphology of the gulf dominated by the Patti Ridge (discussed below; Fig. 4), our profiles (Figs. 7 and 8) show major subvertical faults and numerous small-offset tectonic features with extensional dip slip displacement; these cut the recent sedimentary infill and commonly offset the seafloor. Moreover, the focal mechanisms and the Group-A stress tensor (Fig. 10; Table 1) indicate active extension, supporting an extensional to transtensional kinematic regime for the deformation zone.

Table 1 Seismogenic stress tensors

Group	N	F	R	σ_1		σ_2		σ_3	
				Plunge	Strike	Plunge	Strike	Plunge	Strike
All	268	9.276	0.5	79	337	9	196	7	105
A	120	6.289	0.5	82	339	6	198	5	107
B	10	2.894	0.8	6	193	45	289	44	96
C	19	3.963	0.7	41	162	49	336	3	69
D	20	5.176	0.3	74	205	15	44	5	313

N: Number of events in the group; F: misfit (F < 6°: Homogeneous stress regime; 6°<F<9°: Mostly homogeneous stress regime; F>9°: Heterogeneous stress regime; R: Shape of stress ellipse

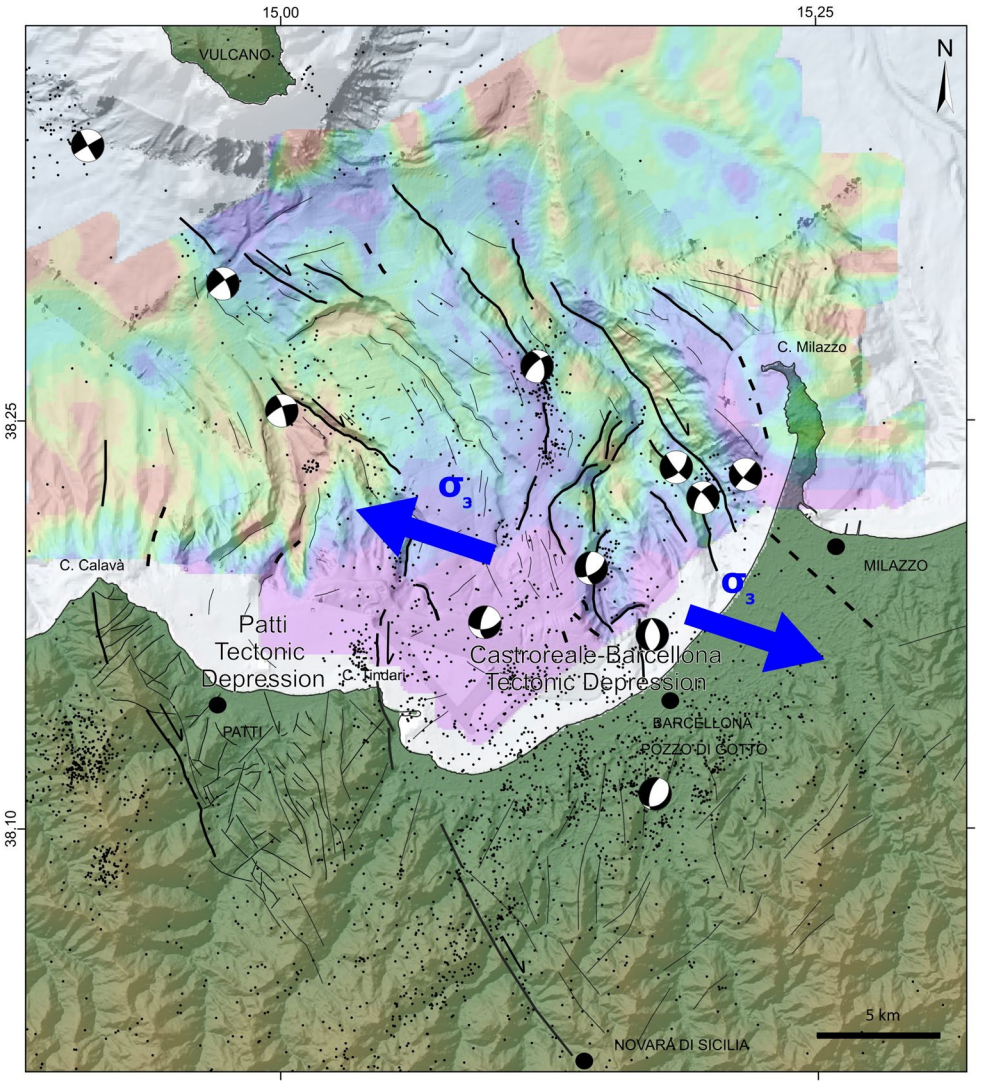

Fig. 11 Tectonic model of the Gulf of Patti, derived from interpretation of all data, including the Cumulative Amplitude Index (CAI) map within the 100–200 ms interval. Shallow seismicity (up to 30 km) and focal mechanisms highlight the transtensional deformation zone extending from the Sicilian coast to the Aeolian islands; blue arrows represent the direction of σ_3 for the group-A events

Previous models proposed an offshore continuation of the Tindari-Letojanni lineament (TLFZ, Fig. 2a, b), toward the Island of Vulcano (Colantoni et al. 2001; Cuppari et al. 1999), while later works do not show a clear offshore counterpart (Argnani et al. 2007; Cultrera et al. 2017a, 2017b; Fig. 2c, d). Our interpretation of seismic and morphostructural data reveals several offshore continuations of major onshore faults controlling the northern Sicilian Tyrrhenian coast (Nigro and Renda 2005; Palano et al. 2015):

- the Tindari-Letojanni fault (ATLFS segment) extends offshore for ~5 km, evidenced by bedrock outcrops on the shelf north of Capo Tindari and by dislocation of the shelf edge (Fig. 4); further north, fault dip inversion suggest that the Tindari-Letojanni segment does not directly connect to the Aeolian archipelago; instead, the ATLFS produces a more complex deformation zone.
- to the east, deformation bounding the eastern flank of the Patti Ridge can be associated with the Vulcano-Milazzo fault (VMF) (Cultrera et al. 2017a); its onshore continuation is not clearly identified (the southernmost sector is highly urbanized), but an anomalous radon degassing zone aligned with the offshore VMF trace supports a fault there (Romano et al. 2023).
- another mapped onshore structure continuing offshore bounds the Capo Calavà ridge (part of the Taormina Fault System (TFS) of Palano et al. (2015); the offshore segment imaged in the profile BC_025 (Fig. 5) appears to accommodate basin-fill tilting with a listric fault geometry, as proposed by Nigro and Renda (2005) from onshore sedimentary succession studies.

The deformation zone crossing the Gulf shows a dominant NW-SE orientation, matching the main trend of the tectonic features mapped offshore and the strike of the longest fault segments located east and west of the Gulf (Fig. 11). We infer a strike-slip component for these fault segments from focal mechanism analysis (Fig. 11) and from morphological

evidence such as lateral displacement of the shelf break along the offshore prolongation of the Tindari-Letojanni fault (Fig. 4).

Conversely, the stress tensor computed for Group-A (Table 1; Fig. 10), centered in the gulf, indicates an extensional tectonic regime with the σ_3 oriented N107°E. This σ_3 orientation matches the strike of onshore tectonic features (Billi et al. 2006; Cultrera et al. 2017a) and offshore structures in the southernmost part of the Gulf, where the primary fault trend and associated morphologies rotate from NW-SE to N-S/NNE-SSW.

The extensional tectonic regime and the rotation of primary tectonic and morphological features are centered in the southern Gulf, where two overlapping major faults exhibit a strike-slip component. These observations, corroborated by the seismological data, support and refine the model of Cultrera et al. (2017a, b), which attributes transtensional deformation in the Castroreale-Barcellona tectonic depression (eastern portion of the Gulf) to a major stepover between two ATLFS segments (Fig. 2d), the Tindari-Novara Fault Zone (TNFZ) and the Vulcano-Milazzo Fault Zone (VMFZ). The right stepover, (e.g., Mia et al. 2024) between two dextral strike-slip fault systems with a gap of about 17 km results in a releasing pull-apart basin.

Integrated morphostructural and seismological analysis constrain the active pull-apart basin to the southeastern sector of the Gulf and its onshore continuation (Castroreale-Barcellona depression), where most earthquakes occur (Fig. 9). The stress regime is consistent with this tectonic framework and the morphology of this portion of the Gulf, characterized by strong erosion driven by two Milazzo Canyon segments (Fig. 4). Seismic profile BC_025 (Fig. 5) indicates that the active pull-apart basin centered on the Castroreale-Barcellona tectonic depression is part of a larger composite basin extending from Capo Calavà to Capo Milazzo. The western part of this composite depression hosts the depocenter of the Plio-Quaternary succession, although the Unit-A1 is slightly thicker between Capo Tindari and Capo Milazzo (Fig. 5). Furthermore, seismicity clusters in the eastern basin while the area west of Capo Tindari is currently seismically quiet (Fig. 11), suggesting an eastward migration of active deformation with tectonic subsidence now focused on the Castroreale-Barcellona depression.

Tectonic model vs. topography

The tectonic model we propose (Fig. 11) integrates our results with previous works (e.g., Cultrera et al. 2017a; and references therein). It shows that the Gulf of Patti is affected by transtensional deformation that creates subsiding depressions, as indicated by fault position and kinematics from 2D and pseudo-3D seismic images, and by the distribution of low-to-moderate magnitude earthquakes and focal mechanisms. Although the Gulf behaves as a releasing pull-apart basin (extensional features in seismic profiles, Figs. 5 and 7; extensional stress from focal mechanism inversion, Fig. 10), its surface morphology is not a simple depression. Instead, the Gulf forms a sill separating the peri-Tyrrhenian Gioia and Cefalù basins (Figs. 1 and 4). This morphology likely results from the interaction of regional and local processes.

The Calabrian Arc is undergoing rapid uplift driven by slab dynamics (Antonioli et al. 2006, 2009; Faccenna et al. 2011; Ferranti et al. 2006). Transtension along the ATLFS induces local subsidence, producing topographic lows such as the Patti and Castroreale-Barcellona tectonic depressions that remain below the sea level. At the same time, the uplift of the Peloritani range drives high erosion rates (Cyr et al. 2010, 2014) and consequent high sediment supply to the basin. Thus, accommodation space produced by competing regional uplift and local subsidence is rapidly filled by sediment aggradation and progradation, which rest unconformably on regional sequence boundaries (Fig. S5). This continuous sedimentation helps explain why the Gulf lacks a pronounced central morphological depression.

However, the combined effect of uplift, subsidence and sedimentation do not fully explain the presence of morphological highs within the Gulf, such as the Patti Ridge, whose origin remains poorly constrained in previous models.

We discuss here three hypotheses for the origin of this morphological feature:

- *Compressive tectonic;* several authors interpret the Patti Ridge as a compressive feature formed by active transpression or a transpressive evolutionary phase of the ATLFS (Argnani et al. 2007; Cuppari et al. 1999). We find no evidence of reverse faults or other compressive structures in the seismic profiles. Furthermore, the stress tensor and the focal mechanisms indicate a prevailing extensional tectonic regime in the Gulf, and the structural high is bounded to the east by active transtensional faults related to the VMF (Fig. 7).
- *Magmatic intrusions*; Cuppari et al. (1999) suggested that the ridge could overlie a magmatic substrate. This hypothesis is consistent with the ridge's position south of the Aeolian Islands along a strike-slip deformation zone that influenced the activity of the archipelago (e.g. Peccerillo et al. 2013). We mapped two deep structures in the seismic profiles that could be magmatic intrusions (Fig. 6, S4). However, limited MCS profiles penetration and the lack of high-resolution magnetic surveys of the Gulf prevents confirmation or rejection of this hypothesis.
- *Extensional tectonic;* given the prevailing extensional stress regime, absence of reverse faults, and considering

the lack of deeper seismic profiles and other geophysical data (such as gravity and magnetics), we consider the extensional tectonic origin the most likely explanation. In this scenario, the Patti Ridge may result from transtension and flexural rebound of the footwall block of a major east-dipping extensional fault, analogous to how the TLF and the TFS bound the Capo Tindari and Capo Calavà ridges (Nigro and Renda 2005).

Tectonic model and geodynamics at the slab edge

The ATLFS has been proposed as the surface expression of the STEP (Subduction-Transform Edge Propagator) fault at the southwestern edge of the Ionian slab (Barreca et al. 2019; Palano et al. 2015; Scarfì et al. 2018). Its main tectonic significance in the Central Mediterranean region began ~ 1-0.7.7 Ma, following a geodynamic reorganization that formed a dextral shear zone separating a compressional belt from an extensional domain (Goes et al. 2004). Several observations support the major role of the ATLFS within the dextral shear zone.

The transtensional character of the main deformation zone in the Gulf likely enhanced local subsidence in an area otherwise dominated by strong uplift associated with dynamic topography (Faccenna et al. 2011), and may explain the asymmetric deposition of the most recent stratigraphic units in the Gulf of Patti (Fig. 5). This transtensional tectonic regime is typical of upper plate deformation at slab edges bounded by a STEP fault, as observed at Gibraltar Arc (Larrey et al. 2023) and the Sulawesi Arc (Komura and Sugimoto 2021), where oblique extension affects the upper plate adjacent to subduction complexes.

The deformation crossing the Gulf also provides migration routes for fluids. We mapped bedrock highs for the first time in the northern portion of the Gulf that are likely linked to Aeolian magmatism, which is strongly connected to the ATLFS (De Astis et al. 2013). Gas seepage are documented offshore and onshore in the study area (Giammanco et al. 2008); seeps near Capo Calavà contain large amounts of mantle-derived volatiles, as indicated by their elevated ^{3}He content (Italiano et al. 2019).

Additionally, seismological data indicate the presence of a deformation zone affecting northeastern Sicily across Capo d'Orlando, Capo Calavà, Capo Tindari and Capo Milazzo. Indeed, the Group-A stress tensor closely matches previous stress tensors for NE Sicily (Neri et al. 2005; Scarfì et al. 2016) and differs from western groups (Groups C and D; Fig. 10). Group C (centered on the deformation zone) appears transtensional, while Group D (to the west) is more extensional, with a slight rotation of principal axes — a rotation also detected with geodetic data (Palano et al. 2015).

Although multiple lines of evidence concur interpreting the ATLFS as a STEP fault, the recent reassessment of the Capo Peloro fault's geodynamic role (Sgroi et al. 2025) raises questions about the relationship between these structures. This complexity likely reflects an active evolving stage of slab necking where a STEP fault can manifest as a broad deformation zone. This evolving tectonic landscape underscores the dynamic nature of the region and the need for continued research to fully understand the interactions between these geological features.

Conclusion

The Aeolian-Tindari-Letojanni Fault System (ATLFS) serves as a critical tectonic transfer zone in the Central Mediterranean region, linking the Sicilian coast to the Aeolian Islands through the Gulf of Patti. This study has highlighted the significance of the ATLFS as a first-order geodynamic structure, characterized by its intense seismicity including moderate to strong historical earthquakes. Our findings reinforce the interpretation of the ATLFS as the shallow expression of the Subduction-Transform Edge Propagator (STEP) fault that marks the southwestern lateral termination of the Calabrian slab.

By compiling a pseudo-3D tectonic model and integrating morpho-bathymetric data, we constrained the position and nature of major active faults in the Gulf of Patti. Our results reveal that the ATLFS forms a complex transtensional deformation zone controlling a composite sedimentary basin. The western sector is best explained as a pull-apart tectonic depression controlled by a right-lateral stepover between two main ATLFS segments. These faults produce localized subsidence that superposes on the regional uplift, reflecting the dynamic interplay of multiscale tectonic processes. By integrating seismological data with the subsurface model, we have successfully recognized a deep transitional domain at crustal and mantle levels that underlies the transtensional deformation zone crossing the Gulf. The presence of a lithospheric structure at deeper crustal levels, likely functioning as a STEP fault, further supports our interpretation of the ongoing tectonic activity in the region.

This study refines the understanding of the neotectonic features in the Gulf of Patti and contributes broader insights into Central Mediterranean geodynamics. Future research should continue to refine our understanding of the ATLFS and its associated fault systems, as well as their implications for seismic hazard assessment in this seismically active region.

Supplementary Information The online version contains supplementary material available at https://doi.org/10.1007/s11001-025-09596-1.

Acknowledgements The authors gratefully acknowledge all the people involved in the research cruises during which the marine geophysical data were acquired. We thank the editor and the reviewers for their insightful comments and suggestions.

Author contributions G. LM. : Writing – original draft, Visualization, Validation, Methodology, Investigation, Formal analysis, Data curation, Conceptualization. L. G. : Writing – original draft, Validation, Software, Methodology, Investigation, Formal analysis, Data curation, Investigation, Conceptualization. T. S. : Writing – original draft, Visualization, Software, Methodology, Investigation, Formal analysis, Data curation. G. B. : Writing – original draft, Software, Visualization, Investigation, Formal analysis, Data curation, Conceptualization. A. P. : Writing – original draft, Formal analysis, Visualization, Validation, Investigation, Conceptualization.

Funding Open access funding provided by Consiglio Nazionale Delle Ricerche (CNR) within the CRUI-CARE Agreement.

Data availability The composite land-sea dataset of 8003 earthquakes occurred from January 2000 to August 2021 is available for download from the INGV repository: https://doi.org/10.13127/styrr_eq3d/2000-2021. The new 268 focal mechanisms computed for this study can be found at: https://doi.org/10.13127/styrr_fm/2000-2021. Marine geoph ysical data are available on request from authors.

Declarations

Competing interests The authors declare no competing interests.

Open Access This article is licensed under a Creative Commons Attribution 4.0 International License, which permits use, sharing, adaptation, distribution and reproduction in any medium or format, as long as you give appropriate credit to the original author(s) and the source, provide a link to the Creative Commons licence, and indicate if changes were made. The images or other third party material in this article are included in the article's Creative Commons licence, unless indicated otherwise in a credit line to the material. If material is not included in the article's Creative Commons licence and your intended use is not permitted by statutory regulation or exceeds the permitted use, you will need to obtain permission directly from the copyright holder. To view a copy of this licence, visit http://creativecommons.org/licenses/by/4.0/.

References

Antonioli F, Ferranti L, Lambeck K, Kershaw S, Verrubbi V, Dai Pra G (2006) Late pleistocene to holocene record of changing uplift rates in Southern Calabria and Northeastern Sicily (southern Italy, central mediterranean Sea). Tectonophysics 422:23–40. https://doi.org/10.1016/j.tecto.2006.05.003

Antonioli F, Ferranti L, Fontana A, Amorosi A, Bondesan A, Braitenberg C, Dutton A, Fontolan G, Furlani S, Lambeck K, Mastronuzzi G, Monaco C, Spada G, Stocchi P (2009) Holocene relative sea-level changes and vertical movements along the Italian and Istrian coastlines. Quat Int 206:102–133. https://doi.org/10.1016/j.quaint.2008.11.008

Argnani A, Serpelloni E, Bonazzi C (2007) Pattern of deformation around the central Aeolian Islands: evidence from multichannel seismics and GPS data. Terra Nova 19:317–323. https://doi.org/10.1111/j.1365-3121.2007.00753.x

Barreca G, Bruno V, Cultrera F, Mattia M, Monaco C, Scarfì L (2014) New insights in the geodynamics of the Lipari–Vulcano area (Aeolian Archipelago, Southern Italy) from geological, geodetic and seismological data. J Geodyn 82:150–167. https://doi.org/10.1016/j.jog.2014.07.003

Barreca G, Scarfì L, Cannavò F, Koulakov I, Monaco C (2016) New structural and seismological evidence and interpretation of a lithospheric-scale shear zone at the Southern edge of the Ionian subduction system (central-eastern Sicily, Italy). Tectonics 35:1489–1505. https://doi.org/10.1002/2015TC004057

Barreca G, Scarfì L, Gross F, Monaco C, De Guidi G (2019) Fault pattern and seismotectonic potential at the south-western edge of the Ionian subduction system (southern Italy): new field and geophysical constraints. Tectonophysics 761:31–45. https://doi.org/10.1016/j.tecto.2019.04.020

Billi A, Barberi G, Faccenna C, Neri G, Pepe F, Sulli A (2006) Tectonics and seismicity of the Tindari fault system, Southern Italy: crustal deformations at the transition between ongoing contractional and extensional domains located above the edge of a subducting slab. Tectonics. https://doi.org/10.1029/2004TC001763

Billi A, Presti D, Faccenna C, Neri G, Orecchio B (2007) Seismotectonics of the Nubia plate compressive margin in the South tyrrhenian region, Italy: clues for subduction inception. Journal of Geophysical Research: Solid Earth. https://doi.org/10.1029/2006JB004837

Billi A, Faccenna C, Bellier O, Minelli L, Neri G, Piromallo C, Presti D, Scrocca D, Serpelloni E (2011) Recent tectonic reorganization of the Nubia-Eurasia convergent boundary heading for the closure of the Western Mediterranean. Bull Soc Geol Fr 182:279–303. https://doi.org/10.2113/gssgfbull.182.4.279

Billi A, Cuffaro M, Orecchio B, Palano M, Presti D, Totaro C (2023) Retracing the Africa–Eurasia nascent convergent boundary in the Western mediterranean based on earthquake and GNSS data. Earth Planet Sci Lett 601:117906. https://doi.org/10.1016/j.epsl.2022.117906

Casetta F, Giacomoni PP, Ferlito C, Bonadiman C, Coltorti M (2020) The evolution of the mantle source beneath Mt. Etna (Sicily, Italy): from the 600 ka tholeiites to the recent trachybasaltic magmas. Int Geol Rev 62:338–359. https://doi.org/10.1080/00206814.2019.1610979

Castello B, Selvaggi G, Chiarabba C, Amato A, Istituto Nazionale di Geofisica e Vulcanologia (INGV) (2006) Catalogo Della sismicità Italiana (CSI) 1981–2002 (Version 1.1). https://doi.org/10.13127/csi.1.1

Catalano S, De Guidi G, Romagnoli G, Torrisi S, Tortorici G, Tortorici L (2008) The migration of plate boundaries in SE sicily: influence on the large-scale kinematic model of the African promontory in Southern Italy. Tectonophysics 449:41–62. https://doi.org/10.1016/j.tecto.2007.12.003

Catalano S, Cirrincione R, Mazzoleni P, Pavano F, Pezzino A, Romagnoli G, Tortorici G (2018) The effects of a Meso-Alpine collision event on the tectono-metamorphic evolution of the peloritani mountain belt (eastern Sicily, Southern Italy). Geol Mag 155:422–437. https://doi.org/10.1017/S0016756817000413

Chizzini N, Artoni A, Torelli L, Basso J, Polonia A, Gasperini L (2022) Tectono-stratigraphic evolution of the offshore Apulian Swell, a continental sliver between two converging orogens (Northern Ionian Sea, central Mediterranean). Tectonophysics 839:229544. https://doi.org/10.1016/j.tecto.2022.229544

Cirrincione R, Fazio E, Fiannacca P, Ortolano G, Pezzino A, Punturo R (2015) The Calabria-Peloritani Orogen, a composite terrane in central Mediterranean; its overall architecture and geodynamic significance for a pre-Alpine scenario around the Tethyan basin. Periodico Di Mineralogia 84:701–749

Colantoni P, Cuppari A, Giovanni G, Morelli D (2001) The Milazzo Canyon and its depositional wedge (submarine fan) on the

Northern Sicilian continental slope (Tyrrhenian Sea). GeoActa (Bologna) 1:15–26

Cultrera F, Barreca G, Burrato P, Ferranti L, Monaco C, Passaro S, Pepe F, Scarfì L (2017a) Active faulting and continental slope instability in the Gulf of Patti (Tyrrhenian side of NE Sicily, Italy): a field, marine and seismological joint analysis. Nat Hazards 86(S2):253–272. https://doi.org/10.1007/s11069-016-2547-y

Cultrera F, Barreca G, Ferranti L, Monaco C, Pepe F, Passaro S, Barberi G, Bruno V, Burrato P, Mattia M, Musumeci C, Scarfì L (2017b) Structural architecture and active deformation pattern in the Northern sector of the Aeolian-Tindari-Letojanni fault system (SE tyrrhenian Sea-NE Sicily) from integrated analysis of field, marine geophysical, seismological and geodetic data. Ital J Geosci 136(3):399–417. https://doi.org/10.3301/IJG.2016.17

Cuppari A, Colantoni P, Gabbianelli G, Morelli D, Alparone R (1999) Assetto ed evoluzione morfostrutturale dell'area marina compresa tra il margine della Sicilia Settentrionale e le Isole Eolie (Golfo di Patti), in: Atti Associazione Italiana Oceanologia Limnologia. pp. 137–149

Cyr AJ, Granger DE, Olivetti V, Molin P (2010) Quantifying rock uplift rates using channel steepness and cosmogenic nuclide–determined erosion rates: examples from Northern and Southern Italy. Lithosphere 2:188–198. https://doi.org/10.1130/L96.1

Cyr AJ, Granger DE, Olivetti V, Molin P (2014) Distinguishing between tectonic and lithologic controls on bedrock channel longitudinal profiles using cosmogenic 10Be erosion rates and channel steepness index. Geomorphology 209:27–38. https://doi.org/10.1016/j.geomorph.2013.12.010

D'Agostino N, Selvaggi G (2004) Crustal motion along the Eurasia-Nubia plate boundary in the Calabrian Arc and Sicily and active extension in the Messina Straits from GPS measurements. Journal of Geophysical Research: Solid Earth. https://doi.org/10.1029/2004JB002998

D'Agostino N, Avallone A, Cheloni D, D'Anastasio E, Mantenuto S, Selvaggi G (2008) Active tectonics of the Adriatic region from GPS and earthquake slip vectors. J Geophys Res Solid Earth 113. https://doi.org/10.1029/2008JB005860

D'Agostino N, D'Anastasio E, Gervasi A, Guerra I, Nedimović MR, Seeber L, Steckler M (2011) Forearc extension and slow rollback of the Calabrian Arc from GPS measurements. Geophys Res Lett 38. https://doi.org/10.1029/2011GL048270

Dahm T, Thorwart M, Flueh ER, Braun T, Herber R, Favali P, Beranzoli L, D'Anna G, Frugoni F, Smriglio G (2002) Ocean bottom seismometers deployed in tyrrhenian sea. Eos Trans AGU 83(29):309–315. https://doi.org/10.1029/2002EO000221

De Astis G, Lucchi F, Dellino P, La Volpe L, Tranne CA, Frezzotti ML, Peccerillo A (2013) Chap. 11 Geology, volcanic history and petrology of Vulcano (central aeolian archipelago). In: Lucchi F, Peccerillo A, Keller J, Tranne CA, Rossi PL (eds) The aeolian Islands volcanoes. Geological Society, London, Memoirs, London, pp 281–349. https://doi.org/10.1144/M37.11

De Guidi G, Lanzafame G, Palano M, Puglisi G, Scaltrito A, Scarfì L (2013) Multidisciplinary study of the Tindari fault (Sicily, Italy) separating ongoing contractional and extensional compartments along the active Africa–Eurasia convergent boundary. Tectonophysics 588:1–17. https://doi.org/10.1016/j.tecto.2012.11.021

Doglioni C, Innocenti F, Mariotti G (2001) Why Mt Etna? Terra Nova 13:25–31. https://doi.org/10.1046/j.1365-3121.2001.00301.x

Doglioni C, Ligi M, Scrocca D, Bigi S, Bortoluzzi G, Carminati E, Cuffaro M, D'Oriano F, Forleo V, Muccini F, Riguzzi F (2012) The tectonic puzzle of the Messina area (Southern Italy): insights from new seismic reflection data. Sci Rep 2:970. https://doi.org/10.1038/srep00970

Fabbri A, Gallignani P, Zitellini N (1981) Geologic evolution of the peri - Tyrrhenian sedimentary basins. In: Wezel FC (ed) Sedimentary basins of mediterranean margins. C.N.R. Italian Project of Oceanography, Bologna, pp 101–126

Faccenna C, Piromallo C, Crespo-Blanc A, Jolivet L, Rossetti F (2004) Lateral slab deformation and the origin of the Western mediterranean arcs. Tectonics. https://doi.org/10.1029/2002TC001488

Faccenna C, Becker TW, Auer L, Billi A, Boschi L, Brun JP, Capitanio FA, Funiciello F, Horvàth F, Jolivet L, Piromallo C, Royden L, Rossetti F, Serpelloni E (2014) Mantle dynamics in the Mediterranean. Rev Geophys 52(3):283–332. https://doi.org/10.1002/2013RG000444

Faccenna C, Molin P, Orecchio B, Olivetti V, Bellier O, Funiciello F, Minelli L, Piromallo C, Billi A (2011) Topography of the Calabria subduction zone (southern Italy): clues for the origin of Mt. Etna. Tectonics. https://doi.org/10.1029/2010TC002694

Ferranti L, Antonioli F, Mauz B, Amorosi A, Dai Pra G, Mastronuzzi G, Monaco C, Orrù P, Pappalardo M, Radtke U, Renda P, Romano P, Sansò P, Verrubbi V (2006) Markers of the last interglacial sea-level high stand along the Coast of italy: tectonic implications. Quat Int 145–146:30–54. https://doi.org/10.1016/j.quaint.2005.07.009

Fröhlich C (1992) Triangle diagrams: ternary graphs to display similarity and diversity of earthquake focal mechanisms. Phys Earth Planet Inter 75:193–198. https://doi.org/10.1016/0031-9201(92)90130-N

Gallen SF, Seymour NM, Glotzbach C, Stockli DF, O'Sullivan P (2023) Calabrian forearc uplift paced by slab–mantle interactions during subduction retreat. Nat Geosci 16:513–520. https://doi.org/10.1038/s41561-023-01185-4

Gamberi F, Casalbore D, Marani M, Rovere M, Bosman A, Calarco M, Dalla Valle G, Leidi E, Martorelli E, Mercorella A, Pierdomenico M, Romagnoli C, Adami C, Falese GF, Fascetti A, Ferrante V, Ingrassia M, Lai E, Montanaro C, Sposato A, Chiocci FL (2024) Geohazard features of the aeolian Island slopes and the North-Eastern Sicily offshore. Journal Maps 20(1). https://doi.org/10.1080/17445647.2024.2343314

Gasperini L, Stanghellini G (2009) SeisPrho: an interactive computer program for processing and interpretation of high-resolution seismic reflection profiles. Comput Geosci 35:1497–1507. https://doi.org/10.1016/j.cageo.2008.04.014

Gasperini L, Ligi M, Stanghellini G (2021) Pseudo-3D techniques for analysis and interpretation of high-resolution marine seismic reflection data. Bull Geophys Oceanogr 62:599–614

Gephart JW (1990) Stress and the direction of slip on fault planes. Tectonics 9(4):845–858. https://doi.org/10.1029/TC009i004p00845

Gephart JW, Forsyth DW (1984) An improved method for determining the regional stress tensor using earthquake focal mechanism data: application to the San Fernando earthquake sequence. J Geophys Res Solid Earth 89(B11):9305–9320. https://doi.org/10.1029/JB089iB11p09305

Ghisetti F (1979) Relazioni Tra strutture e Fasi Trascorrenti e distensive Lungo i sistemi Messina-Fiumefreddo, Tindari-Letojanni e Alia-Malvagna (Sicilia nord-orientale): Uno studio microtettonico. Geol Romana 18:23–58

Giammanco S, Palano M, Scaltrito A, Scarfì L, Sortino F (2008) Possible role of fluid overpressure in the generation of earthquake swarms in active tectonic areas: the case of the peloritani Mts. (Sicily, Italy). J Volcanol Geotherm Res 178(4):795–806. https://doi.org/10.1016/j.jvolgeores.2008.09.005

Gillard D, Wyss M, Okubo P (1996) Type of faulting and orientation of stress and strain as a function of space and time in Kilauea's South flank, Hawaii. J Geophys Res Solid Earth 101(B7):16025–16042. https://doi.org/10.1029/96JB00651

Goes S, Giardini D, Jenny S, Hollenstein C, Kahle HG, Geiger A (2004) A recent tectonic reorganization in the south-central Mediterranean. Earth Planet Sci Lett 226:335–345. https://doi.org/10.1016/j.epsl.2004.07.038

Govers R, Wortel MJR (2005) Lithosphere tearing at STEP faults: response to edges of subduction zones. Earth Planet Sci Lett 236:505–523. https://doi.org/10.1016/j.epsl.2005.03.022

Gutscher M, Dominguez S, de Lepinay BM, Pinheiro L, Gallais F, Babonneau N, Cattaneo A, Le Faou Y, Barreca G, Micallef A, Rovere M (2016) Tectonic expression of an active slab tear from high-resolution seismic and bathymetric data offshore Sicily (Ionian Sea). Tectonics 35:39–54. https://doi.org/10.1002/2015TC003898

Gvirtzman Z, Nur A (1999) The formation of Mount Etna as the consequence of slab rollback. Nature 401:782–785. https://doi.org/10.1038/44555

Henriquet M, Dominguez S, Barreca G, Malavieille J, Monaco C (2020) Structural and tectono-stratigraphic review of the Sicilian orogen and new insights from analogue modeling. Earth-Sci Rev 208:103257. https://doi.org/10.1016/j.earscirev.2020.103257

Italiano F, Bonfanti P, Maugeri SR (2019) Evidence of tectonic control on the geochemical features of the volatiles vented along the Nebrodi-Peloritani Mts (southern Apennine chain, Italy). Geofluids 2019:6250393. https://doi.org/10.1155/2019/6250393

Jolivet L, Baudin T, Calassou S, Chevrot S, Ford M, Issautier B, Lasseur E, Masini E, Manatschal G, Mouthereau F, Thinon I, Vidal O (2021) Geodynamic evolution of a wide plate boundary in the Western Mediterranean, near-field versus far-field interactions. BSGF-Earth Sci Bull 192:48. https://doi.org/10.1051/bsgf/2021043

Komura K, Sugimoto J (2021) Shortcut faults and lateral spreading activated in a Pull-Apart basin by the 2018 palu earthquake, central Sulawesi, Indonesia. Remote Sens. https://doi.org/10.3390/rs13152939

Lanzafame G, Bousquet JC (1997) The Maltese escarpment and its extension from Mt. Etna to Aeolian Islands (Sicily): importance and evolution of a lithosphere discontinuity. Acta Vulcanol 9:113–120

Larrey M, Mouthereau F, Do Couto D, Masini E, Jourdon A, Calassou S, Miegebielle V (2023) Oblique rifting triggered by slab tearing: the case of the Alboran rifted margin in the Eastern betics. Solid Earth 14:1221–1244. https://doi.org/10.5194/se-14-1221-2023

Lentini F, Carbone S (2014) Geology of Sicily. Descriptive Memories of the Geological Map of Italy

Lentini F, Carbone S, Catalano S, Grazzo M (1995) Principali lineamenti strutturali della Sicilia nord-orientale. Studi Geologici Camerti 1995, 319–329

Lofi J, Deverchere J, Gaullier V, Gillet H, Gorini C, Guennoc P, Loncke L, Maillard A, Sage F, Thinon I (2011) Seismic atlas of the Messinian salinity crisis markers in the Mediterranean and Black Sea. Memoire De La Societe Geologique CCGM 179:1–72

Lu Z, Wyss M, Pulpan H (1997) Details of stress directions in the Alaska subduction zone from fault plane solutions. J Geophys Res Solid Earth 102(B3):5385–5402. https://doi.org/10.1029/96JB03666

Lymer G, Lofi J, Gaullier V, Maillard A, Thinon I, Sage F, Chanier F, Vendeville BC (2018) The Western tyrrhenian sea revisited: new evidence for a rifted basin during the Messinian salinity crisis. Mar Geol 398:1–21. https://doi.org/10.1016/j.margeo.2017.12.009

Maesano FE, Tiberti MM, Basili R (2017) The Calabrian arc: three-dimensional modelling of the subduction interface. Sci Rep 7:8887. https://doi.org/10.1038/s41598-017-09074-8

Mia MS, Abdelmeguid M, Harris RA, Elbanna AE (2024) Rupture jumping and seismic complexity in models of earthquake cycles for fault stepovers with off-fault plasticity. Bull Seismol Soc Am 114(3):1466–1480. https://doi.org/10.1785/0120230249

Neri G, Barberi G, Oliva G, Orecchio B (2005) Spatial variations of seismogenic stress orientations in Sicily, South Italy. Phys Earth Planet Inter 148(2–4):175–191. https://doi.org/10.1016/j.pepi.2004.08.009

Neri G, Orecchio B, Totaro C, Falcone G, Presti D (2009) Subduction beneath Southern Italy close the ending: results from seismic tomography. Seismol Res Lett 80:63–70. https://doi.org/10.1785/gssrl.80.1.63

Nigro F, Renda P (2005) Plio-Pleistocene strike-slip deformation in NE Sicily; the example of the area between Capo Calava and Capo Tindari. Ital J Geosci 124:377–394

Palano M, Ferranti L, Monaco C, Mattia M, Aloisi M, Bruno V, Cannavò F, Siligato G (2012) GPS velocity and strain fields in Sicily and Southern Calabria, Italy: updated geodetic constraints on tectonic block interaction in the central Mediterranean. Journal of Geophysical Research: Solid Earth. https://doi.org/10.1029/2012JB009254

Palano M, Schiavone D, Loddo M, Neri M, Presti D, Quarto R, Totaro C, Neri G (2015) Active upper crust deformation pattern along the Southern edge of the tyrrhenian subduction zone (NE Sicily): insights from a multidisciplinary approach. Tectonophysics 657:205–218. https://doi.org/10.1016/j.tecto.2015.07.005

Palano M, Piromallo C, Chiarabba C (2017) Surface imprint of toroidal flow at retreating slab edges: the first geodetic evidence in the Calabrian subduction system. Geophys Res Lett 44:845–853. https://doi.org/10.1002/2016GL071452

Pavano F, Romagnoli G, Tortorici G, Catalano S (2015) Active tectonics along the Nebrodi–Peloritani boundary in northeastern Sicily (Southern Italy). Tectonophysics 659:1–11. https://doi.org/10.1016/j.tecto.2015.07.024

Peccerillo A, De Astis G, Faraone D, Forni F, Frezzotti ML (2013) Chap. 15 compositional variations of magmas in the aeolian arc: implications for petrogenesis and geodynamics. In: Lucchi F, Peccerillo A, Keller J, Tranne CA, Rossi PL (eds) The aeolian Islands volcanoes. Geological Society, London, Memoirs, pp 491–510. https://doi.org/10.1144/M37.15

Polonia A, Torelli L, Artoni A, Carlini M, Faccenna C, Ferranti L, Gasperini L, Govers R, Klaeschen D, Monaco C, Neri G, Nijholt N, Orecchio B, Wortel R (2016) The Ionian and Alfeo–Etna fault zones: new segments of an evolving plate boundary in the central. Mediterranean Sea? Tectonophysics 675:69–90. https://doi.org/10.1016/j.tecto.2016.03.016

Reasenberg P, Oppenheimer DH (1985) FPFIT, FPPLOT and FPPAGE; Fortran computer programs for calculating and displaying earthquake fault-plane solutions. In Open-File Report. U.S. Geological Survey. https://doi.org/10.3133/ofr85739

Romano D, Sabatino G, Magazù S, Di Bella M, Tripodo A, Gattuso A, Italiano F (2023) Distribution of soil gas radon concentration in north-eastern Sicily (Italy): hazard evaluation and tectonic implications. Environ Earth Sci 82:273. https://doi.org/10.1007/s12665-023-10956-6

Rosenbaum G, Lister GS (2004) Neogene and quaternary rollback evolution of the Tyrrhenian Sea, the Apennines, and the Sicilian maghrebides. Tectonics. https://doi.org/10.1029/2003TC001518

Rovida A, Locati M, Camassi R, Lolli B, Gasperini P, Antonucci A (2022) Catalogo parametrico dei terremoti Italiani (CPTI15), versione 4.0. Istituto Nazionale di Geofisica e Vulcanologia (INGV)

Scarfì L, Barberi G, Musumeci C, Patanè D (2016) Seismotectonics of Northeastern Sicily and Southern Calabria (Italy): new constraints on the tectonic structures featuring in a crucial sector for the central mediterranean geodynamics. Tectonics 35:812–832. https://doi.org/10.1002/2015TC004022

Scarfì L, Barberi G, Barreca G, Cannavò F, Koulakov I, Patanè D (2018) Slab narrowing in the central Mediterranean: the Calabro-Ionian subduction zone as imaged by high resolution seismic tomography. Sci Rep 8:5178. https://doi.org/10.1038/s41598-018-23543-8

Selli R, Fabbri A (1971) Tyrrhenian: a Pliocene deep sea, in: Atti Della Accademia Nazionale Dei Lincei. Classe Di Scienze Fisiche, Matematiche e Naturali. Rendiconti. pp. 580–592

Selvaggi G, Chiarabba C (1995) Seismicity and P-wave velocity image of the Southern Tyrrhenian subduction zone. Geophys J Int 121:818–826. https://doi.org/10.1111/j.1365-246X.1995.tb06441.x

Servizio Geologico d'Italia (2011) Carta geologica d'italia Alla scala 1:50.000, Foglio. – Milazzo-Barcellona P.G. ISPRA, Roma, pp 587–600

Servizio Geologico d'Italia (2013) Carta geologica d'italia Alla scala 1:50.000, Foglio 599 – Patti. ISPRA, Roma

Sgroi T, Braun T, Dahm T, Frugoni F (2006) An improved seismicity picture of the Southern tyrrhenian area by the use of OBS and land-based networks: the TYDE experiment. Ann Geophys 49:801–817

Sgroi T, Barberi G, Gasperini L, Govers R, Nijholt N, Lo Mauro G, Ligi M, Artoni A, Torelli L, Polonia A (2025) Structural development and seismogenesis in the Messina Straits revealed by stress/strain pattern above the edge of the Calabrian slab (Central Mediterranean). Tectonophysics 230920. https://doi.org/10.1016/j.tecto.2025.230920

Westaway R (1993) Quaternary uplift of Southern Italy. Journal of Geophysical Research: Solid Earth 98:21741–21772. https://doi.org/10.1029/93JB01566

Working Group ISID (2007) Italian seismological instrumental and parametric database (ISIDe). Istituto Naz Di Geofis E Vulcanologia (INGV). https://doi.org/10.13127/ISIDE

Wyss M, Liang B, Tanigawa WR, Wu X (1992) Comparison of orientations of stress and strain tensors based on fault plane solutions in Kaoiki, Hawaii. J Geophys Res Solid Earth 97(B4):4769–4790. https://doi.org/10.1029/91JB02968

Zhang H, Thurber C, Bedrosian P (2009) Joint inversion for Vp, Vs, and Vp/Vs at SAFOD, Parkfield, California. Geochem Geophys Geosyst. https://doi.org/10.1029/2009GC002709

Zoback ML (1992) First and second order patterns of stress in the lithosphere: the world stress map project. J Geophys Res 97(B8):11703–11728

Publisher's note Springer Nature remains neutral with regard to jurisdictional claims in published maps and institutional affiliations.